Accepted Manuscript

Design, synthesis, docking and QSAR study of substituted benzimidazole linked oxadiazole as cytotoxic agents, EGFR and erbB2 receptor inhibitors

Md Jawaid Akhtar, Anees Ahmad Siddiqui, Ahsan Ahmed Khan, Zulphikar Ali, Rikeshwer Prasad Dewangan, Santosh Pasha, M. Shahar Yar

PII: S0223-5234(16)31020-0

DOI: 10.1016/j.ejmech.2016.12.014

Reference: EJMECH 9105

To appear in: *European Journal of Medicinal Chemistry*

Received Date: 14 October 2016

Revised Date: 22 November 2016

Accepted Date: 6 December 2016

Please cite this article as: M.J. Akhtar, A.A. Siddiqui, A.A. Khan, Z. Ali, R.P. Dewangan, S. Pasha, M.S. Yar, Design, synthesis, docking and QSAR study of substituted benzimidazole linked oxadiazole as cytotoxic agents, EGFR and erbB2 receptor inhibitors, *European Journal of Medicinal Chemistry* (2017), doi: 10.1016/j.ejmech.2016.12.014.

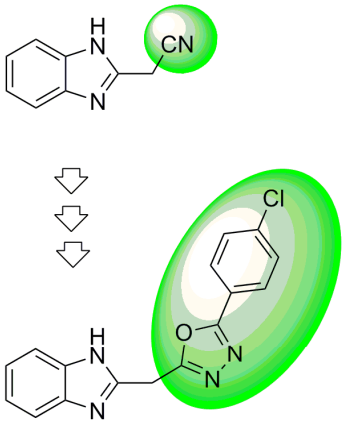

7a; IC_{50} = 5.00 uM (MCF7)
0.081uM(EGFR); 0.61uM(erbB2)

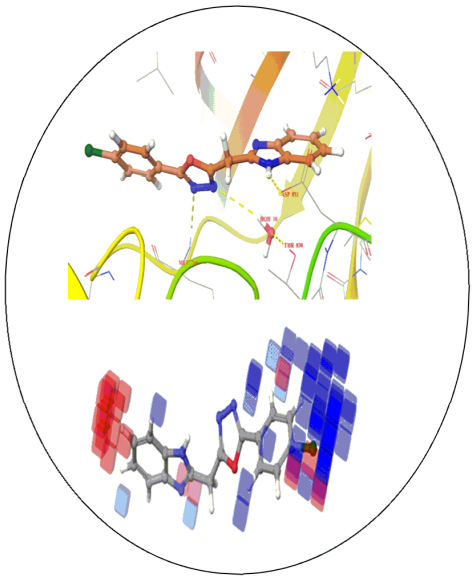

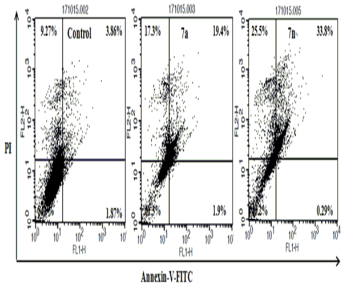

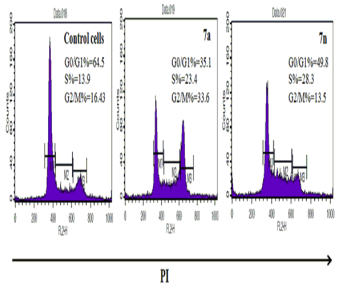

Design, synthesis, docking and QSAR study of substituted benzimidazole linked oxadiazole as cytotoxic agents, EGFR and erbB2 receptor inhibitors

Md Jawaid Akhtar[1], Anees Ahmad Siddiqui[1], Ahsan Ahmed Khan[1], Zulphikar Ali[1], Rikeshwer Prasad Dewangan [2], Santosh Pasha[2] and M Shahar Yar*[1]

[1]*Department of Pharmaceutical Chemistry, Faculty of Pharmacy, Hamdard University, Hamdard Nagar, New Delhi-110062, India*

[2] *Lab no 405, Institute of Genomics and Integrative Biology, New Delhi, India*

**Corresponding Author; E-mail: yarmsy@rediffmail.com*

ABSTRACT:

The synthesis of benzimidazole linked oxadiazole derivatives designed as potential EGFR and erbB2 receptor inhibitors with anticancer and apoptotic activity were studied. Compounds **7a** specifically inhibit EGFR and erbB2 receptor at 0.081 and 0.098 µM concentration. Some of the compounds showed strong, broad-spectrum antiproliferative activitiy when tested against five human cancer cell lines. Compounds **7a** and **7n** were more cytotoxic than 5-fluorouracil against MCF-7 cancer cell, with IC_{50} values of 5.0 and 2.55 µM whereas, only **7a** led to cell cycle arrest at G_2/M phase accompanied by an increase in apoptosis. Compounds **7a** and **7n** showed normal architecture of myofibrils in cardiomyopathy study whereas only compound **7a** showed nearly equal biochemical parameters (SGOT and SGPT) when compared to control. Molecular docking & 3D-QSAR studies were used to establish interactions of **7a** and **7n** within the active site of enzyme for ATP binding site of kinase domain.

Key Words: Benzimidazole linked oxadiazole, Anticancer, Apoptosis, 3D-QSAR studies

1. Introduction

The EGFR (also known as erbB1 or HER1) and the related human epidermal growth factor receptor HER2 (also known as erbB2) is a promising target for anticancer therapy because of its role in tumor growth, metastasis and angiogenesis [1-4, 4a]. Targeted inhibition of this signaling pathway has thereby become attractive therapeutics in cancer treatment and are distinct from the conventional chemotherapy and radiotherapy [3,5]. The EGFR or related receptors are overexpressed, dysregulated or mutated in many epithelial malignancies, and their activation appears important in tumor growth and progression [6, 6a]. Two most clinically advanced approaches for their inhibition includes tyrosine-kinase inhibitors and monoclonal antibodies classes of anticancer therapy [6-8]. The difference exists in that the former functions at the extracellular ligand-binding site, whereas the latter functions at the intracellular tyrosine-kinase domain [6]. Tyrosine-kinase inhibitors compete with the ATP considering the fact that there are so many kinases and all uses ATP as the phosphorylating agent. Thus in the past few years, there has been major focus in the development of ATP-competitive inhibitors [9]. The recently launched kinase inhibitor drugs dasatinib, sunitinib, sorafenib, pazopanib, lapatinib and afatinib inhibit a broad array of cancer-related protein kinases [5, 5a]. These quinazoline-containing derivatives form an important class of synthetic products and represent an attractive scaffold for EGFR and related receptors. However, due to the recent findings of EGFR mutations and erbB2 toxicity-related dose limitation which render the kinase ineffective to Gefitinib, Erlotinib and Afatinib there is an urgent need for new scaffolds to solve this tough problem [9].

Benzimidazoles are structurally related to indole and are ligands for serotonin (5-HT) receptors, histamine (H4) receptors, bradykinin (B2) receptors, and dopamine (D4) receptors [10]. Additionally, benzimidazole being an isostere of purine nucleosides and an important scaffold in various biologically active molecules is widely explored for the development of anticancer agents [11-12]. On the other hand, 1,3,4-oxadiazole heterocycles, recognized as very good bioisosteres of amides and esters, which can contribute substantially in enhancing pharmacological activity by participating in hydrogen bonding interactions with the receptors [13-25]. Some of the drugs under clinical trials containing benzimidazole and oxadiazole moieties and rationally designed targeted compounds are represented in Figure 1**.** In the year 2012 Rashid *et al* [26] synthesized benzimidazole-2-substituted oxadiazole and compounds exhibited remarkable anticancer activity

against most of the tested cell lines with GI_{50} values between 0.79 and 17.8 uM. Salahuddin *et al* in 2014 [27] synthesized benzimidazole-1-oxadiazole derivatives and found compound active against breast cancer cell lines (MDA-MB-468) and showed 72.85 growth percent (GP). Despite many 1-(substituted oxadiazole) benzimidazole derivatives (compound 1, Figure 2) have been synthesized and evaluated for the anticancer and antimicrobial activities [27], 2-(substituted oxadiazole) benzimidazole derivatives (compound 2, Figure 2) have been seldom reported in any literature. The present work is directed towards the design and synthesis of benzimidazole linked oxadiazole derivatives (Figure 3) utilizing easily accessible chemicals, facile synthetic pathways, and evaluation of the EGFR and erbB-2 inhibition assay using gefitinib as a positive control. The literature data concerning EGFR activation have been associated with the development and progression of human tumors viz. breast, liver, lungs and immortalized human keratinocyte. Thus, cytotoxicity studies were determined against five human tumor cell lines (MCF7 "breast", HEPG2 "liver", MDA-MB231 "breast", HaCaT "skin" and A549 "human lung carcinoma" cancers) using MTT assay. Apoptosis, necrosis, and cell cycle analysis were performed using FACS analysis against MCF7 cell lines. Molecular docking studies and 3D-QSAR studies are also performed for understanding the binding and confirming the pharmacological observations.

2. Results and discussion

2.1. Chemistry

As shown in scheme 1, 6-substituted/unsubstituted 2-Cyanomethyl-1H-benzimidazole **(3a-b)** was prepared from refluxing from easily available *o*-phenylenediamine/4-chlorobenzene-1,2-diamine **(1a-b)** and ethyl cyanoacetate **(2)** in anisole for 10h. Compounds **(4a–b)** were synthesized by acidic hydrolysis of 6-substituted/unsubstituted 2-cyanomethyl-1H-benzimidazole **(3a-b)** using benzene sulphonic acid as catalyst. Esterification of the intermediates **(4a-b)** was achieved with ethanol and a catalytic amount of conc. H_2SO_4. The reaction of esters **(5a-b)** with 99% hydrazine monohydrate in ethanol medium produced the corresponding hydrazides **(6a-b)**. The (**7a-x)** and **(8a-e)** derivatives were synthesized by reaction between different substituted aliphatic/aromatic acid with the respective 2-(6-substituted-1H-benzo[d]imidazol-2-yl)acetohydrazide **(6a-b)** in phosphorous oxychloride ($POCl_3$) at 60^{o}C [27]. Heating at temperature above 60°C resulted in breakdown of the

compound **7a** giving two spots in TLC, later characterized into benzimidazole 2-acetyl chloride and benzimidazole 2-acetic acid.

In order to synthesize compounds **(3a-b)**, the reaction of *o*-phenylene diamine with malonic acid/ethyl cyanoacetate in different solvents (4N HCl, 6N HCl, phosphoric acid, PPA, phosphorous oxychloride, potassium carbonate and PCl_3) were carried out. It was found that end product was disappointing mixture of its byproduct under the present experimental conditions. The synthesis of the derivatives **(3a-b)** was optimized using anisole as solvent under refluxing through Dean-Stark apparatus. However, the reaction was incomplete under normal refluxing conditions even at the extended period of time.

Further, synthesis of substituted benzimidazole-2-acetic acid **(4a-b)** was carried out in different media. At first instance, **3a** was hydrolyzed in the presence of conc. sulphuric acid which yielded desired pure product **4a** with 50% yield. In the second stance compound **3a** was hydrolyzed with 15% NaOH followed by neutralization yielded a pure product with 40% yield. Whereas the compound **3a** on hydrolyzing in the presence of benzene sulphonic acid and HCl-Water mixture produced pure compound (92%) in the shortest period of time as compared to other two conventional methods.

2.2. Pharmacology

2.2.1 In vitro EGFR *and erbB2 phosphorylation assay*

Compound **7a** (most active *para* chloro analog) and compound **7n** (active *para* methoxy analog) were tested for their binding affinity to EGFR; both compounds showed better binding to the EGFR. Compounds **7a** (0.081µM) and **7n** (0.098µM) showed comparable EGFR binding affinity as that of the standard drug gefitinib, whereas 2-Cl, 2,4-diCl_2 substituted phenyl **7g** and **7b** and 1-methylnapthyl **7u** contributed moderate inhibition at 4.5, 3.7 & 5.7 µM. Comparing the five analog of 6-chloro benzimidazole derivatives **(8a-e)**, compound **8a** bearing *para* chlorophenyl has the highest binding affinity to the EGFR (0.98 µM). These findings demonstrate that the position and numbers of chlorine affect the EGFR inhibitory activity. Many compounds such as **7k**, **7l**, **7o**, and **7p** were found to be inactive which may be due to the replacement of the phenyl to heteroaromatic rings/aliphatic group. This result demonstrated that phenyl ring was essential for the EGFR bindings. However, substitution in phenyl ring other than chloro/*p*-methoxy groups in compounds **7f, 7i, 7q, 7t, 8c** and **8d** did not exhibit any appreciable activity. Further, compounds having 2,3

$(OCH_3)_2$ (**7j**), and 5-NH_2-2-OH (**7s**) substituted phenyl showed less activity. The inhibitory activities (IC_{50}) of the synthesized compounds are illustrated in Table 1.

Similarly for the selected compounds with significant EGFR activity, it was observed that IC_{50} value for the inhibition of erbB2 was higher than EGFR phosphorylation assay. Among them compound **7a** (0.61uM) displayed the most potent activity, comparable to the positive control geftinib. Compound **7n** (0.91) was also found to be good inhibitor erbB2 autophosphorylation in a MCF7 breast carcinoma cell line engineered to overexpress erbB2 whereas **7b**, **7g** and **7u** were shown to be weak to moderate inhibitor. Alternative 6-chloro benzimidazole derivatives **8a** (IC_{50} = 2.5) showed favorable erbB2 selectivity.

2.2.2 In Vitro Cytotoxicity

The high activity of EGFR signal pathway has been related with an increase in cell proliferation and a poor prognosis in many human malignancies including breast cancer [35-37, 37a], hepatocellular carcinomas [38-40] and 40% to 80% of NSCLC patients [41-45]. Additionally, epidermal growth factor receptor (EGFR), located on the cellular membrane of the keratinocytes, is widely recognized as a key regulator of numerous essential processes underlying skin development, homeostasis, and repair [46]. Abnormalities in the expression and signaling pathways downstream of the epidermal growth factor receptor (EGFR) contribute to malignant transformation in human cancers, including those of the cutaneous epithelium [47]. All these findings indicate targeting EGFR as an effective means to combat breast, liver, lungs and skin cancer.

To verify EGFR and erbB2 receptor tyrosine kinase induced tumorigenesis, *in vitro* MTT assay against five cancer cell lines MCF7 (breast), HaCaT (human skin), MDA-MB231 (breast) HepG2 (liver) and A549 (lung) was performed. The IC_{50} values are reported in Table 1. The three chlorosubstituted phenyl compounds **7a**, **7b** and **8a** showed lower IC_{50} value (5.0µM to 7.0µM) than the 5-FU (7.12µM), this indicates that on introduction of electron rich chloro group at the *para* position of the phenyl ring have contributed better inhibitory activity against MCF7 cancer cell lines. Comparing with the three analogs, compound **7a** with the monosubstituted chloro derivatives at the *para* position of the phenyl ring has the highest inhibition, whereas compound **8a** with additional chloro substitution at 6^{th} position of benzimidazole ring and compound **7b** with 2,4-diCl_2 substitution have lower activity as compared to compound **7a**. Compound **7n** (*para* methoxy)

showed better inhibitory activity with an IC_{50} of 2.5µM as compared to the chloro derivatives analogue against MCF7 cancer cell lines. Compounds **7a**, **7b**, **8a** (chloro derivatives) and **7n** (methoxy derivatives) showed the similar pattern of inhibition against MDA-MB231 cancer cell lines but at higher IC_{50} value (14.5µM to 25.9µM) except for compound **7n** showed better activity with much lower IC_{50} value (0.131µM), this fall in concentration is expected due to the presence of electron donating methoxy group at *p*-position of phenyl ring.

Whereas, the activity against human liver cancer cell line HepG2, compound **8a** was found most active with IC_{50} = 11.2 µM followed by compounds **7a** and **7n** with IC_{50} values of 12.5 and 15.6 µM. The rest of the compounds showed activity at the higher IC_{50} values. Among the tested compounds the order of antitumor activity against the Non-Small Cell Lung Cancer (A549) was **7u** > **7n** > **7a** > **8a** since their IC_{50} values falls between 8.8 to 23.6 µM. Activity against HaCaT cell line revealed that compound **7n** showed higher activity (IC_{50} = 3.8 µM), followed by compound **7a**, **7u** and **8e** with IC_{50} values of 9.5, 12.7 and 19.5 µM respectively. Compound **7a** was more cytotoxic than 5-fluorouracil against MCF-7 cancer cell lines, while **7n** was less active than 5-fluorouracil only against the HepG2 and A549 cancer cell lines.

Structure-activity relationship revealed that the nature of substituent on the C_5-position of the oxadiazole influences the activity. Phenyl ring at C_5-position showed better antitumor activity than the ones with aliphatic chain (**7p)** or heteroaromatic ring (**7k, 7l, 7o, 7v,** and **7w)**. Secondly, an introduction of methyl group between oxadiazole and aromatic ring **7c, 7m, 7u, 7x** and **8c** does not show positive results except compound **7u** which may be due to bulky lipophilic napthyl ring. From the screening results, as shown in (Table 1), it was observed that different substituent on phenyl ring has the varying degree of inhibition against the cancer cell lines. The most active compound of the series **7a** and **7n** suggest that on introduction of electron withdrawing group -Cl and electron donating group -OCH_3 at the *para* position of phenyl ring contributed to anticancer activities, whereas compounds with un-substituted (**7d** and **8d**) causes the anticancer effects but at higher IC_{50}. Compound **7g** and **8e** with *o*-chloro-substituted retains some of the activity in MCF-7, HaCaT, and MDA-MB231 cell lines. Furthermore, when the phenyl ring is disubstituted with -Cl (**7b** and **8b**) retains only its activity against MCF-7 and MDA-MB231 with less active on other cancer cell lines. In the same way, disubstituted -OCH_3 (**7j**) retains activity in all cancer cell lines but at higher IC_{50}. Analogues having *para* substituted –OH (**7f**), -CH_3 (**7i**), -F (**7q**) and *ortho* substituted -CH_3

(**7h**), -$COCH_3$ (**7r**), -COOH (**7t**) showed less cytotoxic activity against all tested cancer cell lines. The introduction of the -Cl group at the 6^{th} position of benzimidazole nucleus (**8a-e**), showed some influence in the antitumor effect but found to be lower as compared with the compounds (**7a-e**).

In general, it was observed that the compounds substituted with chlorine atom/methoxy group at *para* position of aryl ring showed better antitumor activity than the compounds substituted with an aliphatic chain or heteroaromatic ring. Overall, compounds **7a** and **7n** were found active, whereas compound **7n** was most potent in the series which showed highest antitumor activity against MCF-7 and MDA-MB231 cancer cell lines.

2.2.3 Cell Apoptosis

On the basis of EGFR and erbB2 inhibition activity of the compound **7a** and **7n** with broad spectrum activity against the selected cancer cell lines (most potent against MCF7), it was considered worthwhile to further investigate the mechanism of action. To evaluate the apoptosis assay, flow cytometry using propidium iodide (PI) and annexin-V-FITC in MCF7 cells was performed. After post-treatment with the compound **7a** & **7n** at a conc. of 5 µM for 24 h, cells were labeled with the two dyes. The corresponding red (PI) and green (FITC) fluorescence were observed with the flow cytometry. There was increased in the late/secondary cellular apoptosis from 3.86 % (DMSO control) to 19.4 and 33.8 % for compound **7a** and **7n** respectively, whereas there was only marginal increase in the early/primary apoptosis for compound **7a** "i.e." 1.8% (0.1% DMSO control) to 1.9% and corresponding decrease for compound **7n.** These results indicate that compound **7a** act through apoptosis mechanism (Figure 4).

2.2.4 Cell Cycle Inhibition

To understand the effect of selected compound **7a** and **7n** in the cell cycle, FACS analysis was performed. MCF7 cells were treated with the compound 7**a** and **7n** at a concentration of 5 µM each for 24 h. The results confirm 33.6% of cell cycle inhibition in the G_2/M phase (G_2/M arrest) with compound **7a** at a conc. of 5 µM as compared to 16.43% (0.1 % DMSO control), whereas for compound **7n**, the percentage of cells in G_2/M phase was 13.5 % (Figure 5).

2.2.5 Molecular docking

Docking studies were carried out by using ligand docking to understand the binding mode of benzimidazole linked oxadiazole derivatives. To validate the ligand docking, the protein was redocked with the co-crystallized ligand erlotinib. The designed molecules were docked into the active site of EGFR receptor (PDB 1M17) [48-51]. The catalytic domain consists of an N-terminal lobe, which consists mainly of β-strands but contains one α-helix and C helix. The C-terminal lobe is mainly α-helical, and a short strand termed the hinge region connects the two lobes [9]. Figure 6 & 7 (left) give details of the docking analysis of the compound (**7a)**. The results revealed that the N1 of the benzimidazole showed interaction with Asp831. One hydrogen bond was observed between nitrogen of the oxadiazole ring and Met769 and another water molecule mediated hydrogen bond was observed between nitrogen of the oxadiazole ring and Thr830 side chain similar to erlotinib. These interactions highlight the importance of nitrogen atoms for the inhibitory and binding efficiency to EGFR enzymes. The oxadiazole moiety lies in deep hydrophobic pocket and lay in the same site of quinazoline ring of erlotinib. Analysis of compound **7n** binding mode in the active binding site demonstrated that docking mode of compound **7n** is similar to that of compound **7a** with same hydrogen bond between N1 of the benzimidazole and Asp831. The difference lies in the area of oxadiazole ring which do not show hydrogen bond interaction as was seen in compound **7a** and erlotinib. Residues within 2.8 Å areas of erlotinib and benzimidazole linked oxadiazole (**7a & 7n**) are shown in Figure 6 & 7. Figure 8 represent the compound (**7a & 7n**) binding along with the ligand erlotinib inside the protein.

2.2.6 3D QSAR analysis

The scatter plots of the predicted vs. actual inhibitory activity and the contour cubes of the models describe the features essential for the interaction between the synthesized compounds and the EGFR kinase protein. The predicted correlation coefficient (r^2) for the selected model was 0.83 and is shown in Figure 9. The image for the most active compounds **7a** with the favorable (blue cubes) and the unfavorable (red cubes) is presented in Figure 10 a-d. These figures provide the detailed chemical features of the hydrogen bond donor, hydrophobic, electron withdrawing and the combined effects of the substituents of the ligands which contribute to the inhibitory effects against EGFR.

The presence of red cubes in Figure 10a at N3 of benzimidazole and aryl ring attached with the oxadiazole ring showed the unfavorable sites for the hydrogen donor group. Figure 10b showed that

the presence of hydrophobic groups at the benzimidazole ring responsible for the negative potential, whereas addition of suitable hydrophobic groups in the phenyl ring attached to the oxadiazole ring give rise the inhibitory effects against EGFR. In Figure 10c blue cubes to the phenyl ring explain the favorable effects for the electron withdrawing group. The effect of the electron withdrawing substituent at the *para* position of the phenyl group show pronounced inhibitory effects. Figure 10d demonstrate that substitution on phenyl ring is favorable to enhance binding affinity for EGFR whereas, benzimidazole part should be un-substituted. The training set composed 20 members and 9 members of test set with their actual and predicted EGFR kinase activity are presented in Table 2.

2.2.7 Acute oral toxicity

The results showed no mortality in rats when the compound **7a** and **7n** were treated with the dose of 500 mg/kg body weight. Thus, the lethal dose (LD_{50}) of the tested compounds are >500 mg/kg body weight. Therefore, it is concluded that the compounds tested and are classified toxicity oral LD_{50} (>500 <2000 mg/kg) which is recommended by Organization for Economic Co-operation and Development [28].

2.2.8 Cardiomyopathy studies and Hepatotoxicity studies

Cardiotoxicity is a serious side effect of drugs used to treat cancer patients. Cardiac toxicity can be caused by the tyrosine kinase inhibitors imatinib mesylate, dasatinib, nilotinib, sunitinib, sorafenib and lapatinib, while gefitinib and erlotinib have not been related to toxic effect on the heart [53]. Although these drugs are associated with adverse cardiac events (e.g., LV dysfunction [LVD], HF, cardiac ischemia, and myocardial infarction), still granted approval because of the limited treatment options and needs to achieve anticancer efficacy [54]. Therefore, the most potent compounds **7a** and **7n** were further tested for its toxicity in rat (heart) and doxorubicin used as the standard drug. The slide of the treated compounds **7a** & **7n** showed that normal architectures of myofibril in the sub endothelial zone and well maintained architectures of myofibril. There is no significant difference in architecture of cardiac fibre as compared to the normal control group. While group treated with these synthesized compounds were significant altered in architecture of muscle fibre as compared to the doxorubicin (DOX) treated group as shown in Figure 11. DOX control group induced cardiomyopathy, shown by a loss cardiac fibre, vacoulation, inflammation in left ventricle tissue.

Tyrosine kinase inhibitors induce liver injury and liver toxicity which varies in incidence and severity by drugs. Drug induced liver toxicity causes marked increase in SGOT and SGPT levels. The potent compounds (**7a**) when studied for their liver toxic effect showed nearly equal value ($p < 0.01$) of biochemical parameters (SGPT and SGOT) when compared to control whereas compound (**7n**) showed marked increase in the serum hepatic enzyme levels (SGOT and SGPT) (Table 3). Doxorubicin treated animals showed significant increase ($p < 0.01$) in levels of SGOT and SGPT as compared to control [57].

3. Conclusion

A reagent based approach for benzimidazole synthesis coupled with $POCl_3$ cyclization into oxadiazole was used to construct benzimidazole linked oxadiazole. Among the newly synthesized, compounds **7a** inhibit EGFR and erbB2 receptor at 0.081 and 0.61 µM concentration. Moreover, compounds **7a** and **7n** exhibited excellent broad spectrum *in vitro* anticancer activity. The results showed that *p*-substituted chloro/methoxy phenyl at fifth position of oxadiazole (**7a & 7n**) was found to be most active against MCF-7 (2.55-5.00 µM) and MDA-MB231 (0.131-14.5 µM) cancer cell line. Apoptosis assay and cell cycle analysis result demonstrated that compound **7a** inhibits the MCF-7 cancer cells by inducing apoptosis and arresting the cell cycle at G_2/M phase. Furthermore, molecular docking analysis of most active compound **7a** and **7n** in the active site of protein kinase reveals that the binding pattern resembles as that of drug EGFR inhibitor (erlotinib). 3D QSAR study showed the un-substituted benzimidazole ring and phenyl ring substituted with hydrogen-bond donor, hydrophobic, electron withdrawing group is favorable for activity. Additionally, the most active compounds are free from toxicity at a dose ranging from 50 to 500 mg/kg of body weight of animals. Cardiomyopathy studies showed normal architecture of myofibrils for compound **7a** and **7n**, whereas only compound **7a** showed nearly equal biochemical parameters (SGOT and SGPT) as compared to control in hepatoxicity studies. These compounds thus provide the templates and encourage us to continue for further studies to obtain more potent anticancer agents.

4. Experimental section

4.1. General

All the chemicals used were of laboratory grade and procured from E. Merck (Darmstadt, Germany) and S.D. Fine Chemicals (Mumbai, India). Melting points were determined by open capillary tubes in a Hicon melting point apparatus (Hicon, New Delhi, India) and are uncorrected. Purity of the compounds was checked by thin-layer chromatography (TLC) plates (silica gel G), which were visualized by exposing to iodine vapours and UV (ultra violet) light. The FTIR spectra were recorded on (IR affinity SHIMADZU) FTIR spectrophotometer using KBr pellets; υ_{max} values are given in cm^{-1} and The ^1H NMR spectra were taken on a NMR spectra were recorded on Bruker model DRX-400 MHz NMR spectrometer (^1H at 400 MHz, ^{13}C at 100 MHz) in DMSO-d_6. Chemical shifts (δ) are expressed in ppm relative to tetramethylsilane (TMS) as an internal standard and coupling constants (*J* values) are expressed in Hz. Mass spectra were recorded on LCMS/MS (PerkineElmer and LABINDIA, Applied Biosystem) model no. API 3000, presented as m/z. Elemental analysis (C, H and N) were undertaken with Perkin-Elmer model 240C analyzer. Analyses for C, H, N were within ±0.4% of the theoretical values. The absorbance of the *in vitro* assay was measured using an ELISA reader (BioTek Instrument) at a wavelength of 570 nm [28]. The DNA content of the stained cells was analyzed by flow cytometry (BD Biosciences) and the cycle distribution was quantified [29]. Protocol of the apoptosis/necrosis by flow cytometer as per the kit manufacturer's instructions (SIGMA ALDRICH) and *in vitro* EGFR kinase assay by reported procedures [29].

Thin-layer chromatography (TLC) was run throughout the reaction to optimize the reaction for purity and completion. Analytical and spectral data of all the synthesized compounds were in good agreement with the composition of synthesized compounds.

The FT-IR bands at the 3312-3242, 2964-2855, 1689-1626 and 1292-1262 cm^{-1} confirmed the presence of -NH, -CH_2, -C=N and C-O-C functionalities respectively. The ^1H NMR spectrum showed singlet at δ3.65-3.99 and multiplet at δ7.06-8.11 confirming methylene proton and benzimidazole aromatic protons, while broad singlet at δ12.08-12.95 confirms NH of benzimidazole ring protons. The structures and purity of the final compounds were confirmed on the basis of spectral and elemental analyses and the data were within ± 0.4% of the theoretical values. See supplementary material for the general procedure and NMR results for **7a–x** and **8a-e** derivatives.

4.2. General procedure for the synthesis of compounds (3a-b)

A mixture of 1.45 g (0.013mole) of 4-substitutedbenzene-1,2-diamine **(1a-b)** and 1.65g/1.55 ml (0.014mole) of ethylcyanoacetate **(2b)** was heated under reflux for 10h in 6.7 ml (0.061mole). After cooling to room temperature, the precipitate was filtered and washed with anisole. The product was dried and recrystallized with ethanol/water mixture to get compound (**3a)** (88% yield). In the case of chloro-substituted benzene-1,2-diamine **(1b)**, a sticky product was obtained which was extracted with ether to get the pure compound **(3b).**

4.2.1 2-Cyanomethyl-1H-benzimidazole (**3a**, $C_9H_7N_3$) brown; Yield 85%, mp 210-212 ^{0}C; R_f = 0.60 [toluene: ethyl acetate: formic acid (5:4:1)]; IR (KBr) (cm^{-1}): 3383 (NH str), 2253 (C≡N str); ^{1}H NMR (300 MHz, DMSO-*d*$_6$) δ(ppm): 4.37 (s, 2H, -CH_2CN), 7.18 (dd, *J* = 3.0, 3.3 Hz, 2H, H-5,6 benzimidazole), 7.55 (d, 2H, *J* = 8.6 Hz, H-4,7 benzimidazole), 12.63 (bs, 1H, -NH, D_2O exchangeable). ^{13}C NMR (75 MHz, DMSO-*d*$_6$) δ(ppm): 153.88, 138.04, 132.80, 126.54, 122.15, 47.00. Anal. Calcd.: C, 68.78; H, 4.49; N, 26.74; Found: C, 68.75; H, 4.45; N, 26.76.

4.2.2 6-Chloro-2-cyanomethyl-1H-benzimidazole (**3b**, $C_9H_6ClN_3$) brown; Yield 70%, mp 105-106 ^{0}C; R_f = 0.55 [toluene: ethyl acetate: formic acid (5:4:1)]; IR (KBr) (cm^{-1}): 3366 (-NH str), 2215 (-CN); ^{1}H NMR (300 MHz, DMSO-*d*$_6$) δ(ppm): 4.50 (s, 2H, -CH_2CN), 6.67 (d, 1H, *J* = 7.8 Hz, H-5 benzimidazole), 7.07 (d, 1H, *J* = 6.9, H-4 benzimidazole), 7.31 (s, 1H, H-7 benzimidazole), 13.32 (bs, 1H, -NH, D_2O exchangeable). ^{13}C NMR (75 MHz, DMSO-*d*$_6$) δ(ppm): 145.32, 132.43, 131.32, 129.32, 127.16, 123.65, 122.67, 119.21, 41.29. Anal. Calcd.: C, 56.41; H, 3.16; N, 21.93; Found: C, 56.40; H, 3.12; N, 21.96.

4.3 General procedure for the synthesis of compounds (4a-b)

A mixture of 1g of **(3a-b)** and 2 ml of 37% hydrochloric acid in water using 1 ml of benzene sulfonic acid was heated under reflux with stirring for 4-5 h. The reaction was monitored by TLC. Upon completion, reaction mixture was cooled to room temperature, extracted with diethyl ether (3 x 30 ml) and the solvent was removed under reduced pressure to obtain the product **(4a-b)**.

4.3.1 1*H*-Benzimidazol-2-acetic acid (**4a**, $C_9H_8N_2O_2$) green solid; hygroscopic, Yield 81%, mp 240-242 ^{0}C; R_f = 0.42 [toluene: ethyl acetate: formic acid (5:4:1)]; IR (KBr) (cm^{-1}): 3624 (-OH str), 3230(-NH str), 1722 (-C=O str); ^{1}H NMR (300 MHz, DMSO-*d*$_6$) δ(ppm): 3.64 (s, 2H, -C$\underline{H_2}$COOH), 7.58 (dd, 2H, *J* = 7.5, 0.9 Hz, H-5,6 benzimidazole), 7.92 (d, 2H, *J* = 7.5 Hz, H-4,7 benzimidazole), 10.59 (bs, 1H, -COOH), 12.03 (bs, 1H, -NH). ^{13}C NMR (75 MHz, DMSO-*d*$_6$)

δ(ppm): 164.20, 152.20, 131.95, 128.32, 122.50, 48.40. Anal. Calcd.: C, 61.36; H, 4.58; N, 15.90; Found: C, 61.33; H, 4.56; N, 15.92.

4.3.2 6-Chloro-1H-benzimidazol-2-acetic acid (**4b,** $C_9H_7ClN_2O_2$) green solid; Yield 71%, mp 145-147 ^{0}C; R_f = 0.49 [toluene: ethyl acetate: formic acid (5:4:1)]; IR (KBr) (cm^{-1}): 3620 (-OH str), 3235(-NH str), 1720 (-C=O str);^{1}H NMR (300 MHz, DMSO-d_6) δ(ppm): 3.84 (s, 2H, -C<u>H</u>$_2$COOH), 7.06 (d, 1H, *J* = 7.5 Hz, H-5 benzimidazole), 7.35 (d, 1H, *J* = 7.8 Hz, H-4 benzimidazole), 7.64 (s, 1H, H-7 benzimidazole), 11.20 (s, 1H, -COOH), 12.47 (bs, 1H, -NH). ^{13}C NMR (75 MHz, DMSO-d_6) δ(ppm): 164.21, 152.63, 133.24, 132.32, 129.17, 127.13, 123.55, 122.76, 47.24. Anal. Calcd.: C, 51.32; H, 3.35; N, 13.30; Found: C, 51.30; H, 3.32; N, 13.33.

4.4 General procedure for the synthesis of compounds (6a-b)

A solution of compound **(4a-b)** (4g, 0.022 mol) in absolute ethanol (15 mL) was refluxed for 7 h in presence of conc. H_2SO_4 (0.1 mL). After completion of the reaction, it was cooled to room temperature, then 2.14 ml (0.044 mol) of hydrazine hydrate was added and the reaction was further refluxed for another 8h. Detecting single-spot in TLC using the solvent system chloroform: methanol (9:1), the reaction mixture was poured in ice. A precipitate formed **(6a-b)** which was filtered, washed with water and crystallized from ethanol.

4.4.1 2-(1H-benzo[d]imidazol-2-yl)acetohydrazide (**6a**, $C_9H_{10}N_4O$) white flaky; Yield 86%, mp 120-122 ^{0}C; R_f = 0.40 [chloroform: methanol (9:1)]; IR (KBr) (cm^{-1}): 3360 (NH str), 1733 (C=O); ^{1}H NMR (300 MHz, DMSO-d_6) δ(ppm): 3.66 (s, 2H, NH_2), 4.28 (s, 2H, CH_2C=O), 7.11-7.12 (d, 2H, *J* = 3.6, H-5,6 benzimidazole), 7.47 (s, 2H, H-4,7 benzimidazole), 9.36 (s, 1H, -NHNH$_2$), 12.22 (bs, 1H, NH benzimidazole, D_2O exchangeable). ^{13}C NMR (75 MHz, DMSO-d_6) δ(ppm): 164.38, 149.56, 137.68, 133.50, 125.50, 121.27, 45.06. Anal. Calcd.: C, 56.83; H, 5.30; N, 29.46; Found: C, 56.85; H, 5.34; N, 29.43.

4.4.2 2-(6-chloro-1H-benzo[d]imidazol-2-yl)acetohydrazide (**6b**, $C_9H_9ClN_4O$) white flaky; Yield 70%, mp 125-127 ^{0}C; R_f = 0.45 [chloroform: methanol (9:1)]; IR (KBr) (cm^{-1}): 3343 (NH str), 1738 (C=O); ^{1}H NMR (300 MHz, DMSO-d_6) δ(ppm): 3.65 (s, 2H, NH_2), 4.37 (s, 2H, CH_2C=O), 7.15 (s, 1H, H-5 benzimidazole), 7.38 (s, 1H, H-4 benzimidazole), 7.98 (s, 1H, H-7 benzimidazole), 9.28 (s, 1H, -NHNH$_2$), 12.23 (bs, 1H, NH, D_2O exchangeable). ^{13}C NMR (75

MHz, DMSO-d_6) δ(ppm): 165.30, 151.48, 134.30, 133.65, 129.29, 127.16, 123.50, 121.27, 46.60. Anal. Calcd.: C, 48.12; H, 4.04; N, 24.94; Found: C, 48.10; H, 4.08; N, 24.96.

4.5 General procedure for the synthesis of compounds (**7a-x** and **8a-e)**

A mixture of **(6a-b)** (0.001 mol), an aliphatic/aromatic acid (equimolar, 0.001 mol) and $POCl_3$ (5 mL) was heated under reflux along with stirring for 2 h at 60 ^{0}C. After completion of the reaction, checked by single-spot TLC using the solvent systems; chloroform: methanol (9:1), the reaction mixture was cooled and poured slowly onto crushed ice, neutralized with sodium bicarbonate solution. A solid mass precipitated out, which was filtered and washed with excess quantity of water to remove the inorganic component. The compound was recrystallized with ethanol water mixture.

4.5.1 2-((1H-benzo[d]imidazol-2-yl)methyl)-5-(4-chlorophenyl)-1,3,4-oxadiazole (**7a**, $C_{16}H_{11}ClN_4O$) brown; Yield 70%, mp 180-182 ^{0}C; R_f = 0.62 [chloroform: methanol (9:1)]; IR (KBr) (cm^{-1}): 3280 (NH str), 2860 (CH_2 str), 1675, 1669 (C=N str), 1275 (C–O–C str); ^{1}H NMR (300 MHz, DMSO-d_6) δ(ppm): 3.82 (s, 2H, CH_2), 7.13 (dd, 2H, *J* = 1.2, 2.1, H-5,6 benzimidazole), 7.48-7.88 (m, 4H, phe), 7.91 (d, 2H, *J* = 8.7, H-4,7 benzimidazole), 12.36 (bs, 1H, NH, D_2O exchangeable). ^{13}C NMR (75 MHz, DMSO-d_6) δ(ppm): 167.21, 164.96, 149.06, 137.20, 131.57, 130.07, 129.85, 122.62, 121.93, 115.07, 35.02. ESI MS (m/z): 311 [M+H]; Anal. Calcd.: C, 61.84; H, 3.57; N, 18.03; Found: C, 61.80; H, 3.54; N, 18.10.

4.5.2 2-((1H-benzo[d]imidazol-2-yl)methyl)-5-(2,4-dichlorophenyl)-1,3,4-oxadiazole (**7b**, $C_{16}H_{10}Cl_2N_4O$) brown; Yield 68%, mp 140-142 ^{0}C; R_f = 0.71 [chloroform: methanol (9:1)]; IR (KBr) (cm^{-1}): 3267 (NH str), 2855 (CH_2 str), 1689, 1682 (C=N str), 1267 (C–O–C str); ^{1}H NMR (300 MHz, DMSO-d_6) δ(ppm): 3.65 (s, 2H, CH_2), 7.19 (dd, 2H, *J* = 1.5, 2.5, H-5,6 benzimidazole), 7.45-7.85 (m, 3H, phe), 7.90 (d, 2H, *J* = 7.5, H-4,7 benzimidazole), 12.82 (bs, 1H, NH, D_2O exchangeable). ^{13}C NMR (75 MHz, DMSO-d_6) δ(ppm): 168.21, 165.30, 142.62, 136.87, 135.08, 134.76, 133.56, 130.32, 130.00, 128.56, 122.45, 115.25, 34.62. ESI MS (m/z): 345 [M+H]; Anal. Calcd.: C, 55.67; H, 2.92; N, 16.23; Found: C, 55.60; H, 2.96; N, 16.27.

4.5.3 2-((1H-benzo[d]imidazol-2-yl)methyl)-5-benzyl-1,3,4-oxadiazole (**7c**, $C_{17}H_{14}N_4O$) dark brown; Yield 70%, mp 188-190 ^{0}C; R_f = 0.82 [chloroform: methanol (9:1)]; IR (KBr) (cm^{-1}): 3242

(NH str), 2849 (CH_2 str), 1688, 1681 (C=N str), 1284 (C–O–C str); ^{1}H NMR (300 MHz, DMSO-d_6) δ(ppm): 3.89 (s, 2H, CH_2), 3.93 (s, 2H, CH_2-phe), 7.17 (dd, *J* = 1.2, 2.6, 2H, H-5,6 benzimidazole), 7.24-7.59 (m, 5H, phe), 7.73 (d, *J* = 7.8, 2H, H-4,7 benzimidazole), 12.43 (bs, 1H, NH, D_2O exchangeable). ^{13}C NMR (75 MHz, DMSO-d_6) δ(ppm): 165.23, 164.60, 144.52, 139.13, 135.32, 129.64, 128.45, 125.52, 122.43, 117.26, 30.43, 35.48. ESI MS (m/z): 291 [M+H]; Anal. Calcd.: C, 70.33; H, 4.86; N, 19.30; Found: C, 70.36; H, 4.82; N, 19.36.

4.5.4 2-((1H-benzo[d]imidazol-2-yl)methyl)-5-phenyl-1,3,4-oxadiazole (**7d**, $C_{16}H_{12}N_4O$) white flaky; Yield 58%, mp 105-107 ^{0}C; R_f = 0.65 [chloroform: methanol (9:1)]; IR (KBr) (cm^{-1}): 3312 (NH str), 2964 (CH_2 str), 1685, 1674 (C=N str), 1275 (C–O–C str); ^{1}H NMR (300 MHz, DMSO-d_6) δ(ppm): 3.79 (s, 2H, CH_2), 7.21 (dd, 2H, *J* = 1.2, 2.3, H-5,6 benzimidazole), 7.41-7.51 (m, 5H, phe), 7.73 (d, 2H, *J* = 7.5, H-4,7 benzimidazole), 12.42 (bs, 1H, NH, D_2O exchangeable). ^{13}C NMR (75 MHz, DMSO-d_6) δ(ppm): 167.26, 163.56, 143.22, 138.57, 129.53, 128.30, 127.05, 123.45, 123.63, 116.50, 32.99. ESI MS (m/z): 277 [M+H]; Anal. Calcd.: C, 69.55; H, 4.38; N, 20.28; Found: C, 69.59; H, 4.35; N, 20.23.

4.5.5 2-((1H-benzo[d]imidazol-2-yl)methyl)-5-(phenoxymethyl)-1,3,4-oxadiazole (**7e**, $C_{17}H_{14}N4O_2$) flaky and brown; Yield 71%, mp 184-186 ^{0}C; R_f = 0.63 [chloroform: methanol (9:1)]; IR (KBr) (cm^{-1}): 3310 (NH str), 2887 (CH_2 str), 1668, 1659 (C=N str), 1292 (C–O–C str); ^{1}H NMR (300 MHz, DMSO-d_6) δ(ppm): 3.83 (s, 2H, CH_2), 4.66 (s, 2H, CH_2-O-phe), 6.96-7.16 (m, 5H, phe), 7.33 (dd, 2H, *J* = 4.8, 7.5, H-5,6 benzimidazole),7.50 (d, 2H, *J* = 3.3, H-4,7 benzimidazole), 12.35 (bs, 1H, NH, D_2O exchangeable). ^{13}C NMR (75 MHz, DMSO-d_6) δ(ppm): 167.26, 167.12, 166.79, 158.17, 149.01, 129.92, 121.92, 121.25, 115.17, 114.82, 66.36, 34.87. ESI MS (m/z): 307 [M+H]; Anal. Calcd.: C, 66.66; H, 4.61; N, 18.29; Found: C, 66.62; H, 4.67; N, 18.26.

4.5.6 4-(5-((1H-benzo[d]imidazol-2-yl)methyl)-1,3,4-oxadiazol-2-yl)phenol (**7f**, $C_{16}H_{12}N_4O_2$) lt brown; Yield 69%, mp 220-222 ^{0}C; R_f = 0.82 [chloroform: methanol (9:1)]; IR (KBr) (cm^{-1}): 3286 (NH str), 2874 (CH_2 str), 1632, 1626 (C=N str), 1265 (C–O–C str); ^{1}H NMR (300 MHz, DMSO-d_6) δ(ppm): 3.97 (s, 2H, CH_2), 6.51 (s, 1H, -OH), 7.14 (dd, 2H, *J* = 1.5, 2.7, H-5,6 benzimidazole), 6.98-7.48 (m, 4H, phe), 7.86 (d, 2H, *J* = 7.5, H-4,7 benzimidazole),12.77 (bs, 1H, NH, D_2O exchangeable). ^{13}C NMR (75 MHz, DMSO-d_6) δ(ppm): 165.92, 164.58, 145.06, 143.37, 138.10, 122.30, 118.96, 116.95, 116.57, 115.30, 32.25. ESI MS (m/z): 293 [M+H]; Anal. Calcd.: C, 65.75; H, 4.14; N, 19.17; Found: C, 65.79; H, 4.19; N, 19.15.

4.5.7 2-((1H-benzo[d]imidazol-2-yl)methyl)-5-(2-chlorophenyl)-1,3,4-oxadiazole (**7g**, $C_{16}H_{11}ClN_4O$) dark brown; Yield 67%, mp 130-132 ^{0}C; R_f = 0.67 [chloroform: methanol (9:1)]; IR (KBr) (cm^{-1}): 3289 (NH str), 2868 (CH_2 str), 1668, 1659 (C=N str), 1274 (C–O–C str); ^{1}H NMR (300 MHz, DMSO-d_6) δ(ppm): 3.77 (s, 2H, CH_2), 7.06 (dd, 2H, *J* = 1.6, 2.9, H-5,6 benzimidazole), 7.36-7.41 (m, 4H, phe), 7.52 (d, 2H, *J* = 7.6, H-4,7 benzimidazole), 12.22 (bs, 1H, NH, D_2O exchangeable). ^{13}C NMR (75 MHz, DMSO-d_6) δ(ppm): 165.59, 164.12, 142.40, 138.11, 135.69, 132.32, 130.20, 129.54, 128.80, 127.53, 123.66, 117.37, 34.36. ESI MS (m/z): 311 [M+H]; Anal. Calcd.: C, 61.84; H, 3.57; N, 18.03; Found: C, 61.85; H, 3.60; N, 18.09

4.5.8 2-((1H-benzo[d]imidazol-2-yl)methyl)-5-*o*-tolyl-1,3,4-oxadiazole (**7h**, $C_{17}H_{14}N_4O$) white flaky; Yield 68%, mp 190-192 ^{0}C; R_f = 0.82 [chloroform: methanol (9:1)]; IR (KBr) (cm^{-1}): 3267 (NH str), 2889 (CH_2 str), 1672, 1661 (C=N str), 1270 (C–O–C str); ^{1}H NMR (300 MHz, DMSO-d_6) δ(ppm): 2.35 (s, 3H, -CH_3), 3.72 (s, 2H, CH_2), 7.12 (dd, 2H, *J* = 7.5, 10.5, H-5,6 benzimidazole), 7.33-7.38 (m, 4H, phe), 7.66 (d, 2H, *J* = 7.5, H-4,7 benzimidazole), 12.40 (bs, 1H, NH, D_2O exchangeable). ^{13}C NMR (75 MHz, DMSO-d_6) δ(ppm): 165.88, 164.50, 143.23, 138.88, 137.93, 136.15, 129.31, 128.52, 127.50, 126.31, 123.50, 116.91, 33.65. ESI MS (m/z): 291 [M+H]; Anal. Calcd.: C, 70.33; H, 4.86; N, 19.30; Found: C, 70.38; H, 4.89; N, 19.35.

4.5.9 2-((1H-benzo[d]imidazol-2-yl)methyl)-5-*p*-tolyl-1,3,4-oxadiazole (**7i**, $C_{17}H_{14}N_4O$) brown; Yield 65%, mp 164-166 ^{0}C; R_f = 0.85 [chloroform: methanol (9:1)]; IR (KBr) (cm^{-1}): 3292 (NH str), 2895 (CH_2 str), 1677, 1669 (C=N str), 1263 (C–O–C str); ^{1}H NMR (300 MHz, DMSO-d_6) δ(ppm): 2.35 (s, 3H, -CH_3), 3.76 (s, 2H, CH_2), 7.12 (dd, 2H, *J* = 1.5, 2.6, H-5,6 benzimidazole), 7.29-7.90 (m, 4H, phe), 7.95 (d, 2H, *J* = 7.8, H-4,7 benzimidazole), 12.69 (bs, 1H, NH, D_2O exchangeable). ^{13}C NMR (75 MHz, DMSO-d_6) δ(ppm): 166.56, 164.48, 143.65, 138.25, 130.63, 128.61, 127.54, 123.59, 121.58, 116.30, 32.13, 21.33. ESI MS (m/z): 291 [M+H]; Anal. Calcd.: C, 70.33; H, 4.86; N, 19.30; Found: C, 70.36; H, 4.82; N, 19.35.

4.5.10 2-((1H-benzo[d]imidazol-2-yl)methyl)-5-(2,3-dimethoxyphenyl)-1,3,4-oxadiazole (**7j**, $C_{18}H_{16}N_4O_3$) brown; Yield 70%, mp 150-152 ^{0}C; R_f = 0.64 [chloroform: methanol (9:1)]; IR (KBr) (cm^{-1}): 3288 (NH str), 2890 (CH_2 str), 1664, 1651 (C=N str), 1272 (C–O–C str); ^{1}H NMR (300 MHz, DMSO-d_6) δ(ppm): 3.36 (s, 6H, -OCH_3), 3.84 (s, 2H, CH_2), 7.20 (d, 2H, *J* = 6.6, H-4,7 benzimidazole), 7.30-7.37 (m, 3H, phe), 7.52 (dd, 2H, *J* = 2.1, 5.4, H-5,6 benzimidazole), 12.32 (bs, 1H, NH, D_2O exchangeable). ^{13}C NMR (75 MHz, DMSO-d_6) δ(ppm): 165.72, 164.68, 148.35,

145.52, 143.13, 138.52, 130.23, 123.57, 122.62, 120.53, 117.30, 116.29, 52.12, 32.78. ESI MS (m/z): 337 [M+H]; Anal. Calcd.: C, 64.28; H, 4.79; N, 16.66; Found: C, 64.33; H, 4.74; N, 16.70.

4.5.11 2-((1H-benzo[d]imidazol-2-yl)methyl)-5-(thiophen-2-yl)-1,3,4-oxadiazole (**7k**, $C_{14}H_{10}N_4OS$) brown; Yield 55%, mp 110-112 ^{0}C; R_f = 0.71 [chloroform: methanol (9:1)]; IR (KBr) (cm^{-1}): 3273 (NH str), 2868 (CH_2 str), 1678, 1664 (C=N str), 1269 (C–O–C str); ^{1}H NMR (300 MHz, DMSO-d_6) δ(ppm): 3.86 (s, 2H, CH_2), 7.18 (dd, 2H, *J* = 1.8, 2.8, H-5,6 benzimidazole), 7.17-7.73 (m, 3H, thiophene), 7.92 (d, 2H, *J* = 7.6, H-4,7 benzimidazole), 12.76 (bs, 1H, NH, D_2O exchangeable). ^{13}C NMR (75 MHz, DMSO-d_6) δ(ppm): 166.44, 164.49, 143.68, 138.60, 132.42, 131.21, 128.70, 127.70, 123.34, 116.52, 32.90. ESI MS (m/z): 283 [M+H]; Anal. Calcd.: C, 59.56; H, 3.57; N, 19.85; Found: C, 59.51; H, 3.53; N, 19.88.

4.5.12 2-((1H-benzo[d]imidazol-2-yl)methyl)-5-(furan-2-yl)-1,3,4-oxadiazole (**7l**, $C_{14}H_{10}N_4O_2$) brown ; Yield 54%, mp 118-120 ^{0}C; R_f = 0.68 [chloroform: methanol (9:1)]; IR (KBr) (cm^{-1}): 3293 (NH str), 2858 (CH_2 str), 1662, 1655 (C=N str), 1265 (C–O–C str); ^{1}H NMR (300 MHz, DMSO-d_6) δ(ppm): 3.93 (s, 2H, CH_2), 7.13 (dd, 2H, *J* = 7.5, 7.5, H-5,6 benzimidazole), 7.37 (d, 2H, *J* = 7.5, H-4,7 benzimidazole), 7.50-7.68 (m, 3H, furan), 12.26 (bs, 1H, NH, D_2O exchangeable). ^{13}C NMR (75 MHz, DMSO-d_6) δ(ppm): 166.95, 164.62, 147.35, 143.58, 138.93, 138.33, 123.63, 116.69, 116.40, 112.32, 32.72. ESI MS (m/z): 267 [M+H]; Anal. Calcd.: C, 63.15; H, 3.79; N, 21.04; Found: C, 63.19; H, 3.74; N, 21.06.

4.5.13 2-((1H-benzo[d]imidazol-2-yl)methyl)-5-benzhydryl-1,3,4-oxadiazole (**7m**, $C_{23}H_{18}N_4O$) lt brown; Yield 51%, mp 120-122 ^{0}C; R_f = 0.68 [chloroform: methanol (9:1)]; IR (KBr) (cm^{-1}): 3274 (NH str), 2860 (CH_2 str), 1673, 1662 (C=N str), 1262 (C–O–C str); ^{1}H NMR (300 MHz, DMSO-d_6) δ(ppm): 3.65 (s, 2H, CH_2), 4.50 (s, 1H, CH_2-diphenyl), 7.21 (dd, 2H, *J* = 1.8, 2.6, H-5,6 benzimidazole), 7.23-7.53 (m, 10H, diphenyl), 7.86 (d, 2H, *J* = 7.3, H-4,7 benzimidazole), 12.15 (bs, 1H, NH, D_2O exchangeable). ^{13}C NMR (75 MHz, DMSO-d_6) δ(ppm): 166.57, 164.52, 143.72, 143.40, 138.37, 129.67, 128.36, 125.75, 123.44, 116.05, 41.60, 32.42. ESI MS (m/z): 367 [M+H]; Anal. Calcd.: C, 75.30; H, 4.95; N, 15.29 ; Found: C, 75.35; H, 4.93; N, 15.23.

4.5.14 2-((1H-benzo[d]imidazol-2-yl)methyl)-5-(4-methoxyphenyl)-1,3,4-oxadiazole (**7n**, $C_{17}H_{14}N_4O_2$) brown; Yield 72%, mp 160-168 ^{0}C; R_f = 0.80 [chloroform: methanol (9:1)]; IR (KBr) (cm^{-1}): 3263 (NH str), 2883 (CH_2 str), 1667, 1652 (C=N str), 1285 (C–O–C str); ^{1}H NMR (300 MHz, DMSO-d_6) δ(ppm): 3.80 (s, 3H, -OCH_3), 5.02 (s, 2H, CH_2), 7.12-7.15 (dd, 2H, *J* = 3.3, 3.6, H-5,6 benzimidazole), 7.20-7.40 (m, 4H, phe), 7.51 (d, 2H, *J* = 3.3, H-4,7 benzimidazole), 12.35

(bs, 1H, NH, D_2O exchangeable). ^{13}C NMR (75 MHz, DMSO-d_6) δ(ppm): 166.55, 163.94, 162.03, 143.34, 138.70, 123.30, 122.40, 118.63, 116.17, 115.92, 52.08, 32.81. ESI MS (m/z): 307 [M+H]; Anal. Calcd.: C, 66.66; H, 4.61; N, 18.29; Found: C, 66.61; H, 4.65; N, 18.26.

4.5.15 2-((1H-benzo[d]imidazol-2-yl)methyl)-5-(pyridin-3-yl)-1,3,4-oxadiazole (**7o**, $C_{15}H_{11}N_5O$) brown; Yield 67%, mp 160-162 ^0C; R_f = 0.71 [chloroform: methanol (9:1)]; IR (KBr) (cm^{-1}): 3275 (NH str), 2908 (CH_2 str), 1671, 1662 (C=N str), 1272 (C–O–C str); ^1H NMR (300 MHz, DMSO-d_6) δ(ppm): 3.77 (s, 2H, CH_2), 7.12 (dd, 2H, *J* = 7.2, 7.8, H-5,6 benzimidazole), 7.37 (d, 2H, *J* = 7.2, H-4,7 benzimidazole), 7.50-7.68 (m, 4H, pyr), 12.25 (bs, 1H, NH, D_2O exchangeable). ^{13}C NMR (75 MHz, DMSO-d_6) δ(ppm): 166.81, 164.48, 150.09, 147.61, 142.89, 138.29, 134.56, 127.42, 125.42, 123.00, 116.64, 32.70. ESI MS (m/z): 278 [M+H]; Anal. Calcd.: C, 64.97; H, 4.00; N, 25.26; Found: C, 64.92; H, 4.04; N, 25.22.

4.5.16 2-(5-((1H-benzo[d]imidazol-2-yl)methyl)-1,3,4-oxadiazol-2-yl)acetonitrile (**7p**, $C_{12}H_9N_5O$) brown; Yield 65%, mp 145-147 ^0C; R_f = 0.68 [chloroform: methanol (9:1)]; IR (KBr) (cm^{-1}): 3273 (NH str), 2866 (CH_2 str), 1679, 1665 (C=N str), 1282 (C–O–C str); ^1H NMR (300 MHz, DMSO-d_6) δ(ppm): 3.94 (s, 2H, CH_2), 4.21 (s, 2H, CH_2-CN), 7.05 (dd, 2H, *J* = 2.9, 3.5, H-5,6 benzimidazole), 7.76 (d, 2H, *J* = 7.6, H-4,7 benzimidazole), 12.44 (bs, 1H, NH, D_2O exchangeable). ^{13}C NMR (75 MHz, DMSO-d_6) δ(ppm): 165.86, 164.70, 143.40, 138.72, 127.71, 123.32, 116.27, 32.83, 25.34. ESI MS (m/z): 240 [M+H]; Anal. Calcd.: C, 60.25; H, 3.79; N, 29.27; Found: C, 60.20; H, 3.75; N, 29.31.

4.5.17 2-((1H-benzo[d]imidazol-2-yl)methyl)-5-(4-fluorophenyl)-1,3,4-oxadiazole (**7q**, $C_{16}H_{11}FN_4O$) brown; Yield 62%, mp 165-167 ^0C; R_f = 0.66 [chloroform: methanol (9:1)]; IR (KBr) (cm^{-1}): 3269 (NH str), 2902 (CH_2 str), 1688, 1674 (C=N str), 1289 (C–O–C str); ^1H NMR (300 MHz, DMSO-d_6) δ(ppm): 3.81 (s, 2H, CH_2), 7.13 (dd, 2H, *J* = 2.7, 3.0, H-5,6 benzimidazole), 7.29-7.35 (d, 2H, phe), 7.44-7.54 (d, 2H, H-4,7 benzimidazole) 7.91-7.95 (d, 2H, phe), 12.31 (bs, 1H, NH, D_2O exchangeable). ^{13}C NMR (75 MHz, DMSO-d_6) δ(ppm): 166.53, 164.78, 160.90, 143.49, 138.70, 125.33, 123.36, 121.42, 117.61, 116.20, 33.04. ESI MS (m/z): 295 [M+H]; Anal. Calcd.: C, 65.30; H, 3.77; N, 19.04; Found: C, 65.35; H, 3.81; N, 19.09.

4.5.18 1-(2-(5-((1H-benzo[d]imidazol-2-yl)methyl)-1,3,4-oxadiazol-2-yl)phenyl)ethanone (**7r**, $C_{18}H_{14}N_4O_2$) brown; Yield 75%, mp 215-217 ^0C; R_f = 0.64 [chloroform: methanol (9:1)]; IR (KBr) (cm^{-1}): 3289 (NH str), 2852 (CH_2 str), 1662, 1654 (C=N str), 1268 (C–O–C str); ^1H NMR (300 MHz, DMSO-d_6) δ(ppm): 2.31 (s, 3H, -$COCH_3$), 3.87 (s, 2H, CH_2), 7.23 (dd, 2H, *J* = 1.5, 2.7, H-

5,6 benzimidazole), 7.41-7.66 (m, 4H, phe), 7.82 (d, 2H, *J* = 7.6, H-4,7 benzimidazole), 12.30 (bs, 1H, NH, D_2O exchangeable). ^{13}C NMR (75 MHz, DMSO-d_6) δ(ppm): 175.96, 165.96, 164.62, 143.85, 138.91, 137.92, 135.53, 134.21, 133.42, 128.72, 127.30, 122.99, 116.48, 32.70, 29.63. ESI MS (m/z): 319 [M+H]; Anal. Calcd.: C, 67.91; H, 4.43; N, 17.60; Found: C, 67.95; H, 4.48; N, 17.64.

4.5.19 2-(5-((1H-benzo[d]imidazol-2-yl)methyl)-1,3,4-oxadiazol-2-yl)-4-aminophenol (**7s**, $C_{16}H_{13}N_5O_2$) lt brown; Yield 68%, mp 165-167 ^0C; R_f = 0.61 [chloroform: methanol (9:1)]; IR (KBr) (cm^{-1}): 3271 (NH str), 2901 (CH_2 str), 1669, 1661 (C=N str), 1269 (C–O–C str); ^1H NMR (300 MHz, DMSO-d_6) δ(ppm): 3.95 (s, 2H, CH_2), 5.34 (s, 1H, -OH), 6.17 (s, 2H, -NH_2), 6.51-6.69 (m, 3H, phe), 7.12 (dd, 2H, *J* = 1.5, 6.9, H-5,6 benzimidazole),7.34 (d, 2H, *J* = 7.8, H-4,7 benzimidazole), 12.95 (bs, 1H, NH, D_2O exchangeable). ^{13}C NMR (75 MHz, DMSO-d_6) δ(ppm): 166.33, 164.61, 143.75, 143.32, 141.32, 138.92, 123.49, 117.72, 116.76, 116.24, 115.76, 112.80, 32.68. ESI MS (m/z): 308 [M+H]; Anal. Calcd.: C, 62.53; H, 4.26; N, 22.79; Found: C, 62.59; H, 4.29; N, 22.81.

4.5.20 2-(5-((1H-benzo[d]imidazol-2-yl)methyl)-1,3,4-oxadiazol-2-yl)benzoic acid (**7t**, $C_{17}H_{12}N_4O_3$) brown; Yield 75%, mp 176-178 ^0C; R_f = 0.58 [chloroform: methanol (9:1)]; IR (KBr) (cm^{-1}): 3262 (NH str), 2871 (CH_2 str), 1672, 1661 (C=N str), 1285 (C–O–C str); ^1H NMR (300 MHz, DMSO-d_6) δ(ppm): 3.95 (s, 2H, CH_2), 7.19 (dd, 2H, *J* = 3.5, 7.2, H-5,6 benzimidazole), 7.37 (d, 2H, *J* = 7.5, H-4,7 benzimidazole), 7.62-7.85 (m, 4H, phe), 11.42 (s, 1H, -COOH), 12.34 (bs, 1H, NH, D_2O exchangeable). ^{13}C NMR (75 MHz, DMSO-d_6) δ(ppm): 166.72, 165.73, 164.69, 143.70, 138.58, 138.34, 134.54, 130.21, 129.50, 128.15, 127.60, 123.35, 116.65, 32.53. ESI MS (m/z): 321 [M+H]; Anal. Calcd.: C, 63.75; H, 3.78; N, 17.49; Found: C, 63.71; H, 3.72; N, 17.45.

4.5.21 2-((1H-benzo[d]imidazol-2-yl)methyl)-5-(naphthalen-1-ylmethyl)-1,3,4-oxadiazole (**7u**, $C_{21}H_{16}N_4O$) lt brown; Yield 70%, mp 162-164 ^0C; R_f = 0.51 [chloroform: methanol (9:1)]; IR (KBr) (cm^{-1}): 3286 (NH str), 2881 (CH_2 str), 1676, 1668 (C=N str), 1266 (C–O–C str); ^1H NMR (300 MHz, DMSO-d_6) δ(ppm): 3.94 (s, 2H, CH_2), 4.21 (s, 2H, -CH_2), 7.15 (dd, 2H, *J* = 1.9, 2.8, H-5,6 benzimidazole), 7.38 (d, 2H, *J* = 7.6, H-4,7 benzimidazole), 7.65-7.90 (m, 7H, biphenyl), 12.42 (bs, 1H, NH, D_2O exchangeable). ^{13}C NMR (75 MHz, DMSO-d_6) δ(ppm): 166.95, 164.50, 143.44, 138.51, 134.28, 133.05, 132.31, 131.40, 129.32, 128.53, 125.43, 125.16, 117.65, 126.75, 123.42, 116.67, 32.15. ESI MS (m/z): 341 [M+H]; Anal. Calcd.: C, 74.10; H, 4.74; N, 16.46; Found: C, 74.17; H, 4.79; N, 16.51.

4.5.22 2-((1H-benzo[d]imidazol-2-yl)methyl)-5-((2,7a-dihydro-1H-indol-3-yl)methyl)-1,3,4-oxadiazole (**7v**, $C_{19}H_{17}N_5O$) yellow; Yield 68%, mp 180-182 ^{0}C; R_f = 0.56 [chloroform: methanol (9:1)]; IR (KBr) (cm^{-1}): 3267 (NH str), 2872 (CH_2 str), 1672, 1664 (C=N str), 1281 (C–O–C str); ^{1}H NMR (300 MHz, DMSO-d_6) δ(ppm): 3.23 (s, 2H, -CH_2-indole), 3.17-3.43 (m, 3H, pyrrole part of indole), 3.99 (s, 2H, CH_2), 7.01 (bs, 1H, -NH), 7.15 (dd, 2H, *J* = 3.7, 7.2, H-5,6 benzimidazole), 7.38 (d, 2H, *J* = 7.6, H-4,7 benzimidazole), 7.87-7.84 (m, 4H, indole), 12.08 (bs, 1H, NH, D_2O exchangeable). ^{13}C NMR (75 MHz, DMSO-d_6) δ(ppm): 166.47, 164.44, 143.36, 138.21, 138.76, 132.60, 131.32, 123.42, 128.92, 127.44, 116.12, 64.36, 52.13, 32.49, 29.23. ESI MS (m/z): 332 [M+H]; Anal. Calcd.: C, 68.87; H, 5.17; N, 21.13; Found: C, 68.82; H, 5.13; N, 21.19.

4.5.23 2-((1H-benzo[d]imidazol-2-yl)methyl)-5-(pyridin-2-yl)-1,3,4-oxadiazole (**7w**, $C_{15}H_{11}N_5O$) lt brown; Yield 58%, mp 172-174 ^{0}C; R_f = 0.65 [chloroform: methanol (9:1)]; IR (KBr) (cm^{-1}): 3282 (NH str), 2891 (CH_2 str), 1683, 1677 (C=N str), 1268 (C–O–C str); ^{1}H NMR (300 MHz, DMSO-d_6) δ(ppm): 3.84 (s, 2H, CH_2), 7.15 (dd, 2H, *J* = 3.0, 3.3, H-5,6 benzimidazole), 8.67 (d, 2H, *J* = 7.7, H-4,7 benzimidazole), 7.51-8.04 (m, 4H, pyr), 12.23 (bs, 1H, NH, D_2O exchangeable). ^{13}C NMR (75 MHz, DMSO-d_6) δ(ppm): 166.64, 164.32, 157.08, 149.76, 143.03, 138.97, 137.13, 125.30, 123.67, 123.32, 116.14, 32.80. ESI MS (m/z): 278 [M+H]; Anal. Calcd.: C, 64.97; H, 4.00; N, 25.26; Found: C, 64.92; H, 4.04; N, 25.29.

4.5.24 2-((1H-benzo[d]imidazol-2-yl)methyl)-5-(2-methylbenzyl)-1,3,4-oxadiazole (**7x**, $C_{18}H_{16}N_4O$) grey; Yield 70%, mp 181-183 ^{0}C; R_f = 0.70 [chloroform: methanol (9:1)]; IR (KBr) (cm^{-1}): 3272 (NH str), 2878 (CH_2 str), 1665, 1656 (C=N str), 1273 (C–O–C str); ^{1}H NMR (300 MHz, DMSO-d_6) δ(ppm): 2.29 (s, 3H, CH_3), 3.50 (s, 2H, CH_2), 3.81 (s, 2H, CH_2 phenyl), 6.91-7.13 (m, 4H, phe), 7.34 (dd, 2H, *J* = 7.5, 7.8, H-5,6 benzimidazole), 7.61 (d, 2H, *J* = 2.3, H-4,7 benzimidazole), 12.28 (bs, 1H, NH, D_2O exchangeable). ^{13}C NMR (75 MHz, DMSO-d_6) δ(ppm): 166.53, 164.34, 144.87, 138.40, 133.08, 130.93, 127.54, 126.73, 125.43, 123.01, 115.12, 32.43, 30.32, 21.10. ESI MS (m/z): 305 [M+H]; Anal. Calcd.: C, 71.04; H, 5.30; N, 18.41; Found: C, 71.05; H, 5.33; N, 18.45.

4.5.25 2-((6-chloro-1H-benzo[d]imidazol-2-yl)methyl)-5-(4-chlorophenyl)-1,3,4-oxadiazole (**8a**, $C_{16}H_{10}Cl_2N_4O$) brown; Yield 55%, mp 185-187 ^{0}C; R_f = 0.61 [chloroform: methanol (9:1)]; IR (KBr) (cm^{-1}): 3260 (NH str), 2893 (CH_2 str), 1670, 1662 (C=N str), 1279 (C–O–C str); ^{1}H NMR (300 MHz, DMSO-d_6) δ(ppm): 3.97 (s, 2H, CH_2), 6.95 (d, 1H, *J* = 7.5, H-5 benzimidazole), 7.12 (d, 1H, *J* = 7.2, H-4 benzimidazole), 7.34 (s, 1H, H-7 benzimidazole), 7.50-7.67 (m, 4H, phe), 12.21

(bs, 1H, NH, D_2O exchangeable). ^{13}C NMR (75 MHz, DMSO-d_6) δ(ppm): 166.56, 164.34, 143.42, 140.43, 138.37, 132.70, 131.93, 131.31, 129.41, 128.27, 123.32, 116.20, 115.80, 30.70. ESI MS (m/z): 345 [M+H]; Anal. Calcd.: C, 56.84; H, 3.37; N, 15.60; Found: C, 56.79; H, 3.34; N, 15.64.

4.5.26 2-((6-chloro-1H-benzo[d]imidazol-2-yl)methyl)-5-(2,4-dichlorophenyl)-1,3,4-oxadiazole (**8b**, $C_{16}H_9Cl_3N_4O$) brown; Yield 58%, mp 146-148 ^0C; R_f = 0.70 [chloroform: methanol (9:1)]; IR (KBr) (cm^{-1}): 3279 (NH str), 2883 (CH_2 str), 1671, 1664 (C=N str), 1276 (C–O–C str); ^1H NMR (300 MHz, DMSO-d_6) δ(ppm): 3.92 (s, 2H, CH_2), 7.17 (d, 1H, *J* = 7.2, H-5 benzimidazole), 7.55 (d, 1H, *J* = 7.4, H-4 benzimidazole), 7.11-7.70 (m, 3H, phe), 8.11 (s, 1H, H-7 benzimidazole), 12.77 (bs, 1H, NH, D_2O exchangeable). ^{13}C NMR (75 MHz, DMSO-d_6) δ(ppm): 166.57, 164.40, 143.20, 140.86, 138.97, 136.40, 135.29, 132.52, 131.50, 130.53, 129.52, 126.16, 123.81, 116.28, 115.35, 27.70. ESI MS (m/z): 378 [M+H]; Anal. Calcd.: C, 51.87; H, 2.82; N, 14.23; Found: C, 51.82; H, 2.85; N, 14.26.

4.5.27 2-benzyl-5-((6-chloro-1H-benzo[d]imidazol-2-yl)methyl)-1,3,4-oxadiazole (**8c**, $C_{17}H_{13}ClN_4O$) brown; Yield 54%, mp 186-188 ^0C; R_f = 0.85 [chloroform: methanol (9:1)]; IR (KBr) (cm^{-1}): 3306 (NH str), 2872 (CH_2 str), 1689, 1681 (C=N str), 1269 (C–O–C str); ^1H NMR (300 MHz, DMSO-d_6) δ(ppm): 3.80 (s, 2H, CH_2), 3.93 (s, 2H, CH_2-phe), 7.10 (d, 1H, *J* = 7.4, H-5 benzimidazole), 7.26-7.33 (m, 5H, phe), 7.49 (d, 1H, *J* = 7.5, H-4 benzimidazole), 8.11 (s, 1H, H-7 benzimidazole), 12.31 (bs, 1H, NH, D_2O exchangeable). ^{13}C NMR (75 MHz, DMSO-d_6) δ(ppm): 166.32, 164.98, 143.31, 140.53, 138.29, 129.53, 129.20, 128.64, 125.57, 123.31, 116.17, 115.30, 30.08. ESI MS (m/z): 325 [M+H]; Anal. Calcd.: C, 62.87; H, 4.03; N, 17.25; Found: C, 62.82; H, 4.07; N, 17.29.

4.5.28 2-((6-chloro-1H-benzo[d]imidazol-2-yl)methyl)-5-phenyl-1,3,4-oxadiazole (**8d**, $C_{16}H_{11}ClN_4O$) brown; Yield 63%, mp 110-112 ^0C; R_f = 0.64 [chloroform: methanol (9:1)]; IR (KBr) (cm^{-1}): 3294 (NH str), 2883 (CH_2 str), 1671, 1662 (C=N str), 1282 (C–O–C str); ^1H NMR (300 MHz, DMSO-d_6) δ(ppm): 3.78 (s, 2H, CH_2), 7.26 (d, 1H, *J* = 7.5, H-5 benzimidazole), 7.59 (d, 1H, *J* = 7.5, H-4 benzimidazole), 8.12 (s, 1H, H-7 benzimidazole), 7.40-8.21 (m, 5H, phe), 12.82 (bs, 1H, NH, D_2O exchangeable). ^{13}C NMR (75 MHz, DMSO-d_6) δ(ppm): 166.89, 164.83, 143.61, 140.63, 138.64, , 129.50, 129.31, 128.73, 127.56, 123.28, 122.38, 115.98, 115.31, 32.36. ESI MS (m/z): 311 [M+H]; Anal. Calcd.: C, 61.84; H, 3.57; N, 18.03; Found: C, 61.80; H, 3.54; N, 18.07.

4.5.29 2-((6-chloro-1H-benzo[d]imidazol-2-yl)methyl)-5-(2-chlorophenyl)-1,3,4-oxadiazole (**8e**, $C_{16}H_{10}Cl_2N_4O$) brown; Yield 65%, mp 135-137 ^{0}C; R_f = 0.65 [chloroform: methanol (9:1)]; IR (KBr) (cm^{-1}): 3298 (NH str), 2890 (CH_2 str), 1668, 1661 (C=N str), 1290 (C–O–C str); ^{1}H NMR (300 MHz, DMSO-d_6) δ(ppm): 3.67 (s, 2H, CH_2), 7.15 (d, 1H, *J* = 7.6, H-5 benzimidazole), 7.58 (d, *J* = 7.9, 1H, H-4 benzimidazole), 7.18-7.60 (m, 4H, phe), 8.07 (s, 1H, H-7 benzimidazole), 12.42 (bs, 1H, NH, D_2O exchangeable). ^{13}C NMR (75 MHz, DMSO-d_6) δ(ppm): 165.99, 164.87, 143.32, 140.59, 138.48, 138.07, 134.59, 130.62, 129.66, 128.70, 127.15, 126.56, 123.35, 116.64, 115.58, 30.89. ESI MS (m/z): 345 [M+H]; Anal. Calcd.: C, 56.84; H, 3.37; N, 15.60; Found: C, 56.89; H, 3.33; N, 15.64.

4.6 Anticancer activity assays

All of the target compounds were determined against MCF-7 (breast cancer cell line), HaCaT (human skin), MDA-MB231 (breast adenocarcinoma), A549 (human lung carcinoma) and HepG2 (liver hepatocellular carcinoma). Exponentially growing cells were seeded into 96-well plates at a concentration of 3 x 10^3 cells per well. After 24 h incubation at 37 ^{0}C, the culture medium was removed and replaced with fresh medium containing the candidate compounds in different concentrations. The cells were incubated for another 72 h. After 72 h, media of each well was aspirated and added 100 µL of MTT solution (1 mg/mL) in serum free media. The plate was further incubated for 4 h at 37 ^{0}C. Discarded the suspension and added 100 µL of dimethyl sulfoxide (DMSO) to each well and swirled the plates to dissolve the dark blue crystals of formazan. The absorbance was measured using an ELISA reader (BioTek Instrument) at a wavelength of 570 nm. Each concentration was analyzed in triplicate and the experiment was repeated three times. Percentage viability based was calculated based on following formula:

$$\% \text{ cell viability} = 100\ (A\text{-}A_0)/(A_t\text{-}A_0)$$

Where, A represents absorbance of compounds at 570nm and A_0 and A_t represent zero percent cell viability and 100% cell viability determined in media only, respectively.

The average 50% inhibitory concentration (IC_{50}) was calculated after plotting graph of dose-response curves by using GraphPad Prism 5 [28].

4.7 *In vitro* EGFR and erbB2 phosphorylation assay

Exponentially growing KB cells [29] (seeded at $3x10^3$ cells/well in 96-well plates in serum containing medium for 72 h) and then were starved with serum free media for 24 h. Compound was added and incubated for 90 min before the addition of EGF (100 ng/ml) for 5 min to increase EGFR phosphorylation to 90% of max (ED 90) to allow interassay comparison. The cells were lysed in RIRA buffer [50 mmol/L tris (pH 7.4), 1% NP40, 0.25% deoxycholate, 150 mmol/L NaCl, 1 mmol/ L sodium orthovanidate, 1 mmol/L EDTA, and Roche protease inhibitor cocktail] and a sandwich ELISA was used to measure total EGFR phosphorylation.

In Vitro erbB2 phosphorylation studies:- MCF-7 cells were grown in RPMI 1640 containing 10% FCS for 72 h, serum starved (2.5% stripped serum) for 24 h, and incubated with compound for 90 min before stimulating for 5 min with 35 ng/mL (ED90) HRG (Heregulin). Cells were lysed in a radioimmunoprecipitation assay buffer (Sigma radioimmunoprecipitation assay buffer with protease inhibitors) and analyzed using the human phospho-erbB2 ELISA kit (R&D systems). The MCF-7 cl24 line was created by transfecting parental MCF-7 cells with the full-length erbB2 receptor as described previously [29].

4.8 Cell Apoptosis Assay

Cells were seeded at 10^6 per well in 6-well plate and incubated 18 h. Cells were treated with different concentrations of **7a** and **7n** for 24 h and harvested by using trypsin. Cell pellet were washed twice with PBS and cellular apoptosis/necrosis were determined by flow cytometry using annexin V-FITC Apoptosis kit (SIGMA ALDRICH). Protocol of this assay was adopted as per the kit manufacturer's instructions [30].

4.9 Flow Cytometry Cell Analysis

MCF-7 Cells were seeded in density of 10^6 cells per well in 6-well plate and incubated for 18 h. Cells were treated with various concentrations of **7a** and **7n** and incubated further for next 24 h. Cells were washed with PBS and trypsinized to harvest from plates. After washing with PBS fixation of cells was carried out in ice-cold 70% ethanol for 30 min. Cells were resuspended in PBS containing RNase A for 10 min and then added 50 μL PI (500ug/ml) to stain the cellular DNA, the staining process lasted 30 min at 4°C in darkness. The DNA content of the stained cells was

analyzed by flow cytometry (BD Biosciences) and the cycle distribution was quantified. All the experiments were performed in two independent times and representative data are presented here (Figure 5) [30].

4.10 Molecular Docking

The ligand docking studies into tyrosine kinase receptor binding pocket were carried out using Maestro 10.5 program (Schrodinger Inc. USA). The tyrosine kinase enzyme is a validated target for anticancer drug and the crystal structure was downloaded from protein data bank (PDB 1M17) [31]. The protein preparation was done in three step "i.e." preprocess, review & modify and refinement using 'protein preparation wizard' in Maestro 10.5. In these steps, water molecules are deleted and hydrogen atoms are added. The Energy of the structure was minimized using OPLS 2005 force field. Similarly, ligands were prepared again using force field 2005. Receptor grid generation program was run by clicking any atom of the ligand and the default box was prepared. The ligand was docked into the grid generated from the protein using extra precision (XP). The results were evaluated by glide score (docking score) [32].

4.11 3D QSAR generation Model

The primary requirement for the 3D-QSAR generation is the alignment of the molecules. Alignments of the molecules were obtained from running maximum common substructures (Canvas alignment) [33]. Due to the common structural framework of the molecules, atom based 3D-QSAR models were chosen to predict the structure-activity relationships (SAR). Atom based 3D-QSAR were generated for the 20-members of the training set and 9-members of the test set molecules, grid space of 1.0 Å and four PLS factor [34].

4.12 Animal and treatment

The compounds which showed good anticancer activity against cancer cell lines **7a** and **7n** were chosen for the acute toxicity (lethal dose) which is one of the basic requirements in fixing the therapeutic dose in drug development [52]. The investigations were conducted on female albino rats of (110-115 g). The female albino rats were kept under standard conditions at an ambient temperature of 25 ± 2^{o}C and allowed free access to food and water except at the time they were brought out of the cage. Rats were allowed to acclimate to laboratory conditions for 7 days prior to

dosing. All compounds were dissolved in DMSO and administered by gavages at a fixed volume of 0.5 mL/ rats.

4.12.1 Acute toxicity studies

Animals were randomly divided into three groups, five rats of each. Two groups were used for single dose treatments of compounds **7a** and **7n** at 500 mg/kg body weight, and third group as control (0.5 mL DMSO/rat). Then mortality of treated-rats was recorded after 24 h. All the experimental protocols were carried out with the permission from Institutional Animal Ethics committee (IAEC), form no. 1199. Animals were obtained from Central Animal House Facility, Hamdard University, New Delhi-62. Registration no. and date of registration is 173/CPCSEA and Jan 28, 2000.

4.12.2 Cardiomyopathy and Hepatotoxicity studies

Animals were divided into the four groups; the group I and II is treated orally with the drug **7a** and **7n (**500 mg/kg body weight each**)**. Group III was treated orally with a dose (2 mg/kg daily for 5 days for a cumulative dose of 10 mg/kg) of standard drug doxorubicin [55] whereas, group IV serves as control administered with a single dose of DMSO solution. The animals were observed for a periods of 14 days. On the day 14 the animals were sacrificed and the heart were taken out and preserved in 40% of formalin. Section were cut transversally and stained with hematoxylin and eosin before being observed under an Olympus microscope at 100X and 400X magnifications [56].
For the liver enzyme, the active drugs were administered to each animal at a single dose treatment of compounds **7a** and **7n** at 500 mg/kg body weight. After the stipulated period of 2 weeks, each animal was anesthetized by anesthetic ether, and blood was collected from the liver to assess the biochemical parameters such as SGOT, SGPT, alkaline phosphate, and total protein according to the reported methods [58].

Acknowledgments

We are grateful to Jamia Hamdard (Hamdard University) for providing laboratory facilities. One of the author (Md. Jawaid Akhtar, IF-130481) expresses thanks to Department of Science and Technology (DST) New Delhi, India for INSPIRE fellowship. Authors also expresses their thanks to All India Council for Technical Education (AICTE) New Delhi, India for RPS (8-

99/RIFD/RPS/POLICY-3/2013-14) fellowship. Assistance provided by Vaibhav Jain and Adarsh from CSIR- IGIB in FACS analysis thankfully acknowledged. Support rendered by Vinod Devaraji and Pritesh Bhat of schrodinger is also acknowledged.

Abbreviation: QSAR, Quantitative structure-activity relationships; SGOT, Serum glutamic oxaloacetic transaminase; SGPT, serum glutamic-pyruvic transaminase; ATP, Adenosine triphosphate; NSCLC, Non-small cell lung cancer; MTT, 3-(4,5-Dimethylthiazol-2-yl)-2,5-Diphenyltetrazolium Bromide; PPA, polyphosphoric acid; 5-FU, 5-Flurouracil; FACS, Fluorescence-activated cell sorting; LVD, Left ventricular dysfunction; HF, Heart Failure; $POCl_3$, phosphorus oxychloride; FTIR, Fourier transform infrared spectroscopy; KBr, Potassium Bromide; ELISA, enzyme-linked immunosorbent assay; ^1H NMR, Proton nuclear magnetic resonance; TLC, Thin layer chromatography; HCl, Hydrochloric acid; NaOH, Sodium hydroxide; PBS, Phosphate-buffered saline.

References

1. J.J Liao, Molecular recognition of protein kinase binding pockets for design of potent and selective kinase inhibitors, J. Med. Chem. 50 (2007) 409-424.
2. J. Zhang, P.L Yang, Gray NS, Targeting cancer with small molecule kinase inhibitors, Nature reviews/cancer, 9 (2009) 28-39.
3. F. Zuccotto, E. Ardini, E. Casale, M. Angiolini, Through the "Gatekeeper Door": Exploiting the active kinase conformation, J. Med. Chem. 53 (2010) 2681-2694.
4. R.B Bakr, E.K.A. Abdelall, M.K. Abdel-Hamid, M.M. Kandeel, Design and synthesis of new EGFR-tyrosine kinase inhibitors containing pyrazol0[3-4-d] pyrimidine cores as anticancer agents, Bull. Pharm. Sci. Assiut. Univ. 35 (2012) 27-42. [4a] J. Han, S. Henriksen, K.G. Nørsett , E. Sundby , B.H. Hoff, Balancing potency, metabolic stability and permeability in pyrrolopyrimidine-based EGFR inhibitors, Eur. J. Med. Chem. 124 (2016) 583-607.
5. R. Determann, J. Dreher, K. Baumann, L. Preu, P.G. Jones, F. Totzke, C. Schächtele, M.H.G. Kubbutat, C. Kunick, 2-Anilino-4-(benzimidazol-2-yl)pyrimidines - A multikinase inhibitor scaffold with antiproliferative activity toward cancer cell lines, Eur. J. Med. Chem. 53 (2012) 254-263. [5a] J. Han, S.J. Kaspersen, S. Nervik, K.G. Nørsett, E. Sundby, B. H. Hoff, Chiral 6-aryl-furo[2,3-d]pyrimidin-4-amines as EGFR inhibitors, Eur. J. Med. Chem. 119 (2016) 278-299.
6. P.M. Harari, Epidermal growth factor receptor inhibition strategies in oncology, Endocrine-Related Cancer, 11 (2004) 689–708. [6a] S. Yin, C. Tang, B. Wang, Y. Zhang, L. Zhou, L. Xue, C. Zhang, Design, synthesis and biological evaluation of novel EGFR/HER2 dual inhibitors bearing a oxazolo[4,5-g]quinazolin-2(1H)-one scaffold. Eur. J. Med. Chem. 120 (2016) 26-36.
7. M. Zukin, Epidermal growth factor receptor inhibitors in non-small cell lung cancer: current status and future perspectives, Rev. Assoc. Med. Bras. 58 (2012) 263-268.
8. A. Díaz, A. Lage, Therapies based on inhibitors of the epidermal growth factor receptor: reaching for the future, Biotecnología. Aplicada. 24 (2007)10-18.

9. J. Lin, W. Shen, J. Xue, J. Sun, X. Zhang, C. Zhang, Novel oxazolo[4,5-g]quinazolin-2(1H)-ones: Dual inhibitors of EGFR and Src protein tyrosine kinases, Eur. J. Med. Chem. 55 (2012) 39-48.
10. L. Chen, C. Chang, D.B. Salunke et al, Divergent Synthesis of Unsymmetrical Annulated Biheterocyclic Compound Libraries: Benzimidazole Linked Indolo-benzodiazepines/quinoxaline, ACS. Comb. Sci. 13 (2011) 391–398.
11. A. Kamal, P.P. Kumar, K. Sreekanth et al, Synthesis of new benzimidazole linked pyrrolo[2,1-c][1,4]benzodiazepine conjugates with efficient DNA-binding affinity and potent cytotoxicity, Bioorg. Med. Chem. Lett. 18 (2008) 2594–2598.
12. K. Shao, X. Zhang, P. Chen et al, Synthesis and biological evaluation of novel pyrimidine-benzimidazol hybrids as potential anticancer agents, Bioorg. Med. Chem. Lett. 24 (2014) 3877-3881.
13. N.C. Desai, N. Bhatt, H. Somani, A. Trivedi, Synthesis, antimicrobial and cytotoxic activities of some novel thiazole clubbed 1,3,4-oxadiazoles, Eur. J. Med. Chem. 67 (2013) 54-59.
14. D. Kumar, G. Patel, A.K. Chavers, K. Chang, K. Shah, Synthesis of novel 1,2,4-oxadiazoles and analogues as potential anticancer agents, Eur. J. Med. Chem. 46 (2011) 3085-3092.
15. N.B. Patel, A.C. Purohit, D.P. Rajani, R. Moo-Puc, G. Rivera, New 2-benzylsulfanyl-nicotinic acid based 1,3,4-oxadiazoles: Their synthesis and biological evaluation, Eur. J. Med. Chem. 62 (2013) 677-687.
16. N.I. Ziedan, F. Stefanelli, S. Fogli, A.D. Westwell, Design, synthesis and pro-apoptotic antitumour properties of indole-based 3,5-disubstituted oxadiazoles, Eur. J. Med. Chem. 45 (2010) 4523-4530.
17. M.A. Ali, M. Shaharyar, Oxadiazole mannich bases: synthesis and antimycobacterial activity, Bioorg. Med. Chem. Lett. 17 (2007) 3314-16.
18. R. Gitto, S. Ferro, S. Agnello et al, Synthesis and evaluation of pharmacological profile of 1-aryl-6,7-dimethoxy-3,4-dihyroisoquinoline-2(1H)-sulfonamide, Bioorg. Med. Chem. 17 (2009) 3659-3664.
19. A. Zarghi, M. Faizi, B. Shafaghi et al. Design and synthesis of new 2-substituted-5-(2-benzylthiophenyl)-1,3,4-oxa diazole as benzodiazepine receptor agonists, Bioorg. Med. Chem. Letters. 15 (2009) 3126-3129.

20. D. Dewangan, A. Pandey, T. Sivakumar et al, Synthesis of some novel 2,5-disubstituted 1,3,4-oxadiazole and its analgesic, anti-inflammatory, anti-bacterial and anti-tubercular activity, Int. J. Chemtech. Res. 3 (2010) 1397-1412.
21. A.G. Banerjee, N. Das, S.A. Shengule et al, Synthesis, characterization, evaluation and molecular dynamics studies of 5, 6–diphenyl–1,2,4–triazin–3(2H)–one derivatives bearing 5–substituted 1,3,4–oxadiazole as potential anti–inflammatory and analgesic agents, Eur. J. Med. Chem. 101 (2015) 81-95.
22. S. Rapolu, M. Alla, V.R. Bommena et al, Synthesis and biological screening of 5-(alkyl(1H-indol-3-yl))-2-(substituted)-1,3,4-oxadiazoles as antiproliferative and anti-inflammatory agents, Eur. J. Med. Chem. 66 (2013) 91-100.
23. M.Y. Wani, A. Ahmad, R.A. Shiekh, K.J. Al-Ghamdi, A.J.F.N. Sobral, Imidazole clubbed 1,3,4-oxadiazole derivatives as potential antifungal agents, Bioorg. Med. Chem. 23 (2015) 4172-4180.
24. A.K.M. Iqbal, A.Y. Khan, M.B. Kalashetti, N.S. Belavagi, Y. Gong, I.A.M. Khazi, Synthesis, hypoglycemic and hypolipidemic activities of novel thiazolidinedione derivatives containing thiazole/triazole/oxadiazole ring, Eur. J. Med. Chem. 53 (2012) 308-315.
25. M.B. Palkar, A.S. Singhai, P.M. Ronad et al, Synthesis, pharmacological screening and in silico studies of new class of Diclofenac analogues as a promising anti-inflammatory agents, Bioorg. Med. Chem. 22 (2014) 2855-2866.
26. M. Rashid, A. Husain, R. Mishra. Synthesis of benzimidazoles bearing oxadiazole nucleus as anticancer agents, Eur. J. Med. Chem. 54 (2012) 855-866.
27. Salahuddin , M. Shaharyar, A. Mazumder, M.J. Ahsan, Synthesis, characterization and anticancer evaluation of 2-(naphthalen-1-ylmethyl/naphthalen-2-yloxymethyl)-1-[5-(substituted phenyl)-[1,3,4]oxadiazol-2-ylmethyl]-1H-benzimidazole, Arab. J. Chem. 7 (2014) 418-424.
28. Y. Duan, Y. Ma, E. Zhang et al, Design and synthesis of novel 1,2,3-triazole-dithiocarbamate hybrids as potential anticancer agents, Eur. J. Med. Chem. 62 (2013)11-19.
29. D.M. Hickinson, T. Klinowska, G. Speake et al, AZD8931, an Equipotent, Reversible Inhibitor of Signaling by Epidermal Growth Factor Receptor, ERBB2 (HER2), and ERBB3: A Unique Agent for Simultaneous ERBB Receptor Blockade in Cancer, Clin. Cancer. Res. 16 (2010) 1159−1169.

30. Y. Duan, Y. Zheng, X. Li et al. Design, synthesis and antiproliferative activity studies of novel 1,2,3-triazole-dithiocarbamate-urea hybrids, Eur. J. Med. Chem. 64 (2013) 99-110.
31. J. Stamos, M.X. Sliwkowski, C. Eigenbrot, Structure of the epidermal growth factor receptor kinase domain alone and in complex with a 4-anilinoquinazoline inhibitor, J. Biol. Chem. 277 (2002) 46265-46272.
32. M.N. Noolvi, H.M. Patel, M. Kaur, Benzothiazoles: Search for anticancer agents, Eur. J. Med. Chem. 54 (2012) 447-462.
33. S. Kalva, D. Vinod, L.M. Saleena, Field- and Gaussian-based 3D-QSAR studies on barbiturate analogs as MMP-9 inhibitors, Med. Chem. Res. 22 (2013) 5303-5313.
34. R. Chekkara, N. Kandakatla, V.R. Gorla, S.R. Tenkayala et al, Theoretical studies on benzimidazole and imidazo[1,2-a]pyridine derivatives as Polo-like kinase 1 (Plk1) inhibitors: Pharmacophore modeling, atom-based 3D-QSAR and molecular docking approach, J. Saudi. Chem. Soc. xx (2014) xxx-xxx.
35. R. Garcia, R.A. Franklin, J.A. McCubrey, Cell Death of MCF-7 Human breast cancer cells induced by EGFR activation in the absence of other growth factors, Cell. Cycle. 5 (2006) 1840-1846.
36. H.W. Lo, S.C. Hsu, M.C. Hung, EGFR signaling pathway in breast cancers: from traditional signal transduction to direct nuclear translocalization, Breast. Cancer. Res. Treat. 95 (2006) 211-218.
37. M.K. Wendt, W.K. Williams, P.E. Pascuzzi et al, The antitumorigenic function of EGFR in metastatic breast cancer is regulated by expression of Mig6, Neoplasia. 17 (2015) 124-133. [37a] K.M. Amin, F.F. Barsoum, F.M. Awadallah, N.E. Mohamed, Identification of new potent phthalazine derivatives with VEGFR-2 and EGFR kinase inhibitory activity, Eur. J. Med. Chem. 123 (2016) 191-201.
38. P. Zhao, X. Yang, S. Qi et al, Molecular Imaging of Hepatocellular Carcinoma Xenografts with Epidermal Growth Factor Receptor Targeted Affibody Probes, Bio. Med. Res. Int. (2013) 1-11.
39. R. Kannangai, F. Sahin, M.S. Torbenson, EGFR is phosphorylated at Ty845 in hepatocellular carcinoma, Modern. Path. 19 (2006) 1456–1461.

40. K. Hoffmann, Z. Xiao, C. Franz, E. Mohr et al, Involvement of the epidermal growth factor receptor in the modulation of multidrug resistance in human hepatocellular carcinoma cells in vitro, Cancer. Cell. Int. (2011) 1-9.
41. S.V. Schaeybroeck, J. Kyula, D.M. Kelly et al, Chemotherapy-induced epidermal growth factor receptor activation determines response to combined gefitinib/chemotherapy treatment in non–small cell lung cancer cells, Mol. Cancer. Ther. 5 (2006) 1154-1165.
42. J.A. Engelman, P.A. Janne, C. Mermel et al, ErbB-3 mediates phosphoinositide 3-kinase activity in gefitinib-sensitive non-small cell lung cancer cell lines, P.N.A.S. 102 (2005) 3788–3793.
43. N. Li, H. Li, F. Su et al, Relationship between epidermal growth factor receptor (EGFR) mutation and serum cyclooxygenase-2 Level, and the synergistic effect of celecoxib and gefitinib on EGFR expression in non-small cell lung cancer cells, Int. J. Clin. Exp. Pathol. 8 (2015) 9010-9020.
44. J. Zhang, X. Pan, I.A. Astsaturov et al, Relationship of Aurora-A kinase and EGFR inhibition in non-small cell lung cancer (NSCLC) cell lines, J. Clin. Oncol. ASCO Annual Meeting Abstracts. (2011) 29.
45. M. Ono, A. Hirata, T. Kometani et al, Sensitivity to gefitinib (Iressa, ZD1839) in non-small cell lung cancer cell lines correlates with dependence on the epidermal growth factor (EGF) receptor/extracellular signal-regulated kinase 1/2 and EGF receptor/Akt pathway for proliferation, Mol. Cancer. Ther. 3 (2004) 465-472.
46. M. Cichocki, H. Szaefer, V. Krajka-Kuzniak et al, The effect of resveratrol and its methylthio-derivatives on EGFR and Stat3 activation in human HaCaT and A431 cells, Mol. Cell. Biochem. 396 (2014) 221–228.
47. C.J. Barnes, R. Bagheri-Yarmand, M. Mandal et al, Suppression of Epidermal Growth Factor Receptor, Mitogenactivated Protein Kinase, and Pak1 Pathways and Invasiveness of Human Cutaneous Squamous Cancer Cells by the Tyrosine Kinase Inhibitor ZD1839 (Iressa). Mol. Cancer. Ther. 2 (2003) 345–351.
48. M.A. Abdelgawad, R.B. Bakr, O.A. Alkhoja et al, Design, synthesis and antitumor activity of novel pyrazolo[3,4-d]pyrimidine derivatives as EGFR-TK inhibitors, Bioorg. Chem. 66 (2016) 88–96.

49. X. Tao, Y. Duan, Chen. L et al, Design, synthesis and biological evaluation of pyrazolylnitroimidazole derivatives as potential EGFR/HER-2 kinase inhibitors, Bioorg. Med. Chem. Lett. 26 (2016) 677–683.
50. B. Barlaam, J. Anderton, P. Ballard et al, Discovery of AZD8931, an Equipotent, Reversible Inhibitor of Signaling by EGFR, HER2, and HER3 Receptors, ACS Med. Chem. Lett. 4 (2013) 742−746.
51. Y. Qian, H. Zhang, H. Zhang et al, Synthesis, molecular modeling, and biological evaluation of cinnamic acid, Bioorg. Med. Chem. 18 (2010) 4991–4996.
52. M.A. Abu-Zaied, E.M. El-Telbani, G.H. Elgemeie, G.A.M. Nawwar, Synthesis and in vitro anti-tumor activity of new oxadiazole thioglycosides, Eur. J. Med. Chem. 46 (2011) 229-235.
53. G.S. Orphanos, G.N. Ioannidis, A.G. Ardavanis, Cardiotoxicity induced by tyrosine kinase inhibitors. Acta. Oncologica. 48 (2009) 964-970.
54. H.R. Mellor, A.R. Bell, J. Valentin, R.R.A. Roberts, Cardiotoxicity Associated with Targeting Kinase Pathways, Cancer. Toxicological. Sciences, 120 (2011) 14–32.
55. R.A. Jensen, E.M. Acton , J.H. Peters, Doxorubicin cardiotoxicity in the rat: comparison of electrocardiogram, transmembrane potential, and structural effects, J. Cardiovasc. Pharmacol. 6 (1984)186-200.
56. M. Rashid, A .Husain, M. Shaharyar, R. Mishra, A. Hussain, O. Afzal, Design and synthesis of pyrimidine molecules endowed with thiazolidin-4-one as new anticancer agents, Eur. J. Med. Chem, 83 (2014) 630-645.
57. C.F. Spraggs, C.F. Xu, C.M. Hunt, Genetic Characterization to Improve Interpretation and Clinical Management of Hepatotoxicity Caused by Tyrosine Kinase Inhibitors. Pharmacogenomics, 14 (2013) 541-554.
58. J.T.Litchfield, F.A. Wilcoxon , A simplified method of evaluating dose-effect experiments. J Pharmacol Exp Ther 96 (1949) 99–113.

Scheme caption

Scheme 1. Synthesis of intermediate and target compounds.

Figure captions

Figure 1. Drugs under clinical trials containing benzimidazole and oxadiazole with other heterocyclic scaffolds and rationally designed targeted compounds.

Figure 2. The structures of two different benzimidazole substituted oxadiazole

Figure 3. Design of the proposed molecule

Figure 4. Apoptosis effect in MCF-7 cancer cell line detected with Annexin V-FITC/PI double staining post treatment with compound **(7a)** and (**7n)** at 24 h interval at a dose of 5 µM. Lower left quadrant represents live cells, lower right quadrant is for early/primary apoptotic cells, upper right quadrant is for late/secondary apoptotic cells and upper left quadrant represent the necrotic cells.

Figure 5. DNA content by flow cytometry in MCF-7 cancer cell line of compound (**7a)** and (**7n)** of 5µM dose concentration at 24 h interval after fixing and staining with PI.

Figure 6. Schematic diagram of the interaction made by compound (**7a)** (left) and (**7n)** (right) with the kinase domain of EGFR enzyme (PDB code 1M17), hydrogen bonds are indicated as pink dotted line. Compound (**7a)** is showing hydrogen bond interaction with Met769, Asp831 and water molecule mediated hydrogen bond interaction between oxadiazole nitrogen and Thr830 similar to erlotinib. Similarly, Compound **(7n)** lacking the hydrogen bond interaction of the oxadiazole ring but preserving the hydrogen bond interaction with Asp831 similar to that of compound **(7a)**.

Figure 7. Binding mode of compound (**7a)** (left) and (**7n)** (right) into the kinase domain of EGFR (PDB code 1M17) showing hydrogen bond interaction with Met769, Asp831 and water molecule mediated hydrogen bond interaction between oxadiazole nitrogen and Thr830 (**7a)** and one hydrogen bond with Asp831(compound **7n**).

Figure 8. Binding mode of compound (**7a)** (left) and (**7n)** (right) with the ligand erlotinib into the kinase domain of EGFR (PDB code 1M17).

Figure 9. Predicted IC_{50} (EGFR TK) values vs the experimental IC_{50} (EGFR TK).

Figure 10. Effects of various substituent shown by the 3D QSAR; (a) hydrogen-bond donor, (b) hydrophobic (c) electron withdrawing (d) combined effect. In figure red cubes showed the unfavorable substituents effects and the blue cubes for the favorable substituents.

Figure 11. **A**: Effects of compound **7a** showing normal architecture of cardiac fibre. **B**: Effects of compound **7n** showing normal architecture of cardiac fibre. **C**: Photomicrograph showing effects of normal control on cardiac fibre (well maintained architecture of myofibrils) **D**: Effects of Doxorubicin showing cardiomyopathy shown by loss of cardiac fiber, vacoulation and inflammation in left ventricle tissue.

JAMIA HAMDARD
(HAMDARD UNIVERSITY)
(Declared as Deemed-to-be University under Section 3 of the UGC Act, 1956 vide Notification No. F.9-16/88-U.3 dated 10.5.1989 of the Government of India)
Accredited by NAAC in 'A' Category

Phones : 011-26059688 (12 Lines)
Extns. : 5590, 5595
Fax : 011 26059663
E-mail : cahf@jamiahamdard.ac.in
Website : www.jamiahamdard.edu

HAMDARD NAGAR
NEW DELHI - 110062

CENTRAL ANIMAL HOUSE FACILITY

Dr. A.K. Tiwari
Veterinary Officer

Approval of Jamia Hamdard Animal Ethics Committee
Project Proposal Number 1199

10.11.2016

Registration No. of JHAEC: -	173/GO/Re/S/2000/CPCSEA
Chief Investigator: -	Dr. M. Shahar Yar
Department and Faculty: -	Pharmaceutical Chemistry, Pharmacy
Title of the Project: -	"Design and synthesis of benzimidazole derivatives as anticancer agents"
Animal Approved: -	27 Female Wistar Rat
Date of Approval: -	10.11.2015
Date of Initiation of Project: -	7.3.2013
Date of Completion of Project: -	7.3.2016

Dr. A. K. Tiwari
Member Secretary/ V.O., CAHF
Jamia Hamdard

Dr. A. K. Tiwari
Veterinary Officer/In-Charge
Central Animal House Facility
Hamdard University (Jamia Hamdard)
Hamdard Nagar, New Delhi-110062

Table 1. Inhibitory results of substituted benzimidazole linked oxadiazole derivatives against five human cancer cell lines and *in vitro* EGFR and erbB2 phosphorylation assay.

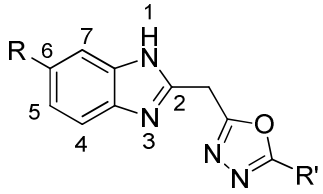

Comp.	R	R'	IC_{50} (uM)[a,b]						
			EGFR	erbB2	MCF7	HaCaT	MDA-MB231	HepG2	A549
7a	H	4-Cl $-C_6H_4-$	0.081	0.61	5.0	9.5	14.5	12.5	15.2
7b	H	2,4-Cl_2-C_6H_3-	3.7	4.7	7.0	23.2	25.9	52.7	52.6
7c	H	C_6H_5-CH_2-	25.0	36.9	26.3	75.3	29.8	51.2	61.4
7d	H	C_6H_5-	31.8	40.0	59.0	57.5	50.4	65.4	64.7
7e	H	C_6H_5-O-CH_2-	46.3	52.4	32.4	61.0	35.5	45.2	42.5
7f	H	4-OH-C_6H_4-	>100	ND	32.7	65.9	35.6	85.3	ND
7g	H	2-Cl-C_6H_4-	4.5	6.5	22.3	25.3	21.2	63.7	>100
7h	H	2-CH_3-C_6H_4-	39.7	46.8	52.2	64.7	50.0	>100	ND
7i	H	4-CH_3-C_6H_4-	>100	ND	24.6	67.9	29.8	83.4	ND
7j	H	2,3$(OCH_3)_2$-C_6H_3-	61.0	>100	35.2	55.3	52.3	35.4	31.0
7k	H	2-Thiophene	>100	ND	62.1	>100	65.3	>100	ND
7l	H	2-Furan	>100	ND	56.3	>100	>100	55.7	ND
7m	H	$(C_6H_5)_2$-CH_2-	45.0	57.6	42.8	65.3	48.6	63.2	54.1
7n	H	4-OCH_3-C_6H_4-	0.098	0.91	2.5	3.8	0.131	15.6	13.2
7o	H	3-Pyridine	>100	ND	75.9	>100	86.7	>100	ND
7p	H	-CH_2CN	>100	ND	80.5	>100	92.3	>100	>100
7q	H	4-F-C_6H_4	>100	ND	30.2	31.2	32.4	51.2	ND
7r	H	2-$COCH_3$-C_6H_4-	65.4	ND	52.3	73.9	51.6	63.2	61.3
7s	H	5-NH_2- 2-OH-C_6H_3-	70.0	ND	51.1	55.3	50.3	73.2	65.2
7t	H	2-COOH-C_6H_4-	>100	ND	39.3	65.7	31.8	81.0	35.7

7u	H	Napthyl-CH_2-	5.7	8.8	27.5	12.7	13.2	25.0	8.8
7v	H	3-Indole	86.2	ND	69.7	68.9	55.2	>100	>100
7w	H	2-Pyridine	73.5	ND	54.2	>100	53.6	>100	56.2
7x	H	2-CH_3-C_6H_4-CH_2-	50.0	ND	42.3	>100	47.3	>100	60.0
8a	-Cl	4-Cl-C_6H_4-	0.98	2.5	5.6	24.4	14.7	11.2	23.6
8b	-Cl	2,4-Cl_2-C_6H_3-	45.1	52.6	30.4	75.6	29.9	52.3	50.0
8c	-Cl	C_6H_5-CH_2-	>100	ND	24.7	32.7	29.8	55.7	ND
8d	-Cl	C_6H_5-	>100	ND	65.4	82.7	71.2	82.3	ND
8e	-Cl	2-Cl-C_6H_4-	33.2	45.7	25.7	19.5	26.5	32.7	45.4
5-FU	----	-------	-----	-----	7.12	-----	5.0	5.0	1.16
Geftinib	----	-------	0.011	0.024					

[a]Antiproliferative activity was assayed by exposure for 72 h to substances and expressed as concentration required to inhibit tumor cell proliferation by 50% (IC_{50}).
[b]i*n vitro* EGFR and erbB2 phosphorylation assay by exposure for 90 min to the test compounds and results are expressed as IC_{50}.
ND = not determined

Table 2. The experimental and predicted inhibitory activity against EGFR of compounds (**7a-x**, **8a-e**) by 3D-QSAR models.

Comp[a].	EGFR		Residual error
	Actual pIC_{50}	Predicted pIC_{50}	
7a	7.092	5.4761	-1.615
7b	5.432	5.3046	-0.127
7c	4.602	4.2195	-0.382
7d	4.498	4.4094	-0.088
7e	4.334	4.8756	0.5412
7f	4.0	4.3283	0.3283
7g	5.347	4.4094	-0.9373
7h	4.401	4.3729	-0.0282
7i	4.0	5.3346	1.3346
7j	4.215	4.8480	0.6333
7k	4.0	3.8788	-0.1211
7l	4.0	3.8038	-0.1961
7m	4.347	4.2156	-0.1311
7n	7.009	6.3014	-0.7073
7o	4.0	4.0111	0.0111
7p	4.0	3.6034	-0.3965
7q	4.0	4.9668	0.9668
7r	4.184	4.3729	0.1885
7s	4.155	4.1324	-0.0224
7t	4.0	3.6946	-0.3053
7u	5.244	5.4269	0.1827
7v	4.064	4.094	0.0297
7w	4.134	3.846	-0.2871
7x	4.301	4.177	-0.1234
8a	6.009	5.476	-0.5325
8b	4.346	5.288	0.9421
8c	4.0	4.157	0.1570
8d	4.0	4.409	0.4094
8e	4.479	4.409	-0.0694

[a] The underlined compounds indicate for the test set and rest are represented as training.

Table 3. Effects of most active compounds on levels of enzyme transaminases in liver function test.

Compounds[a]	SGOT ± SEM	SGPT ± SEM
7a	38.57 ± 1.86	24.19 ± 2.70
7n	110.91 ± 2.37**	94.26 ± 1.85**
Control[b]	34.18 ± 1.53	27.73 ± 1.42

[a]Relative to control and data were analyzed by ANOVA followed by Student's *t*-test for n = 6 at $^{**}p < 0.01$

[b] Control group was treated with 0.5% methyl cellulose for 15 days.

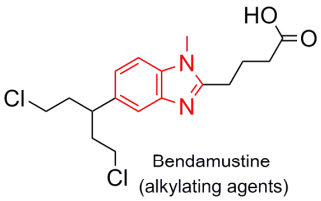

Bendamustine
(alkylating agents)

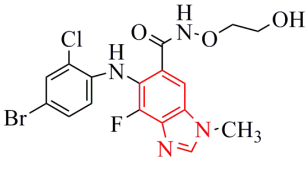

Selumetinib
Mitogen-activated protein kinase kinase(MEK)

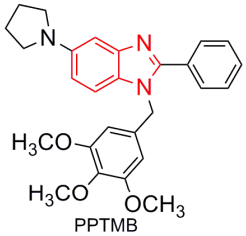

PPTMB
(Prostrate cancer cells)

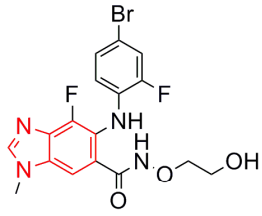

Binimetinib (MEK phase III)

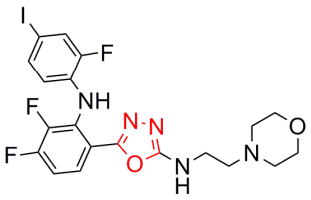

PD 334581 (MEK 1)

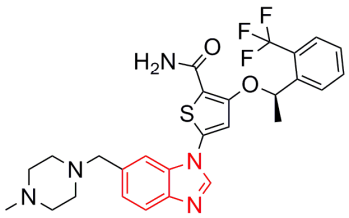

GSK461364 (PLK inhibitor)

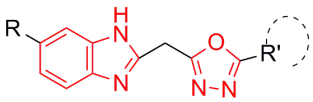

(7a-x), (8a-e)

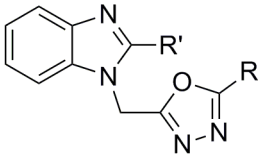

(1)

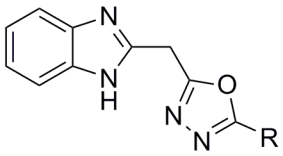

(2)

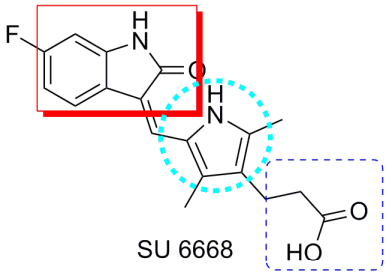

SU 6668

PDGFR, VEGFR and FGFR inhibitor

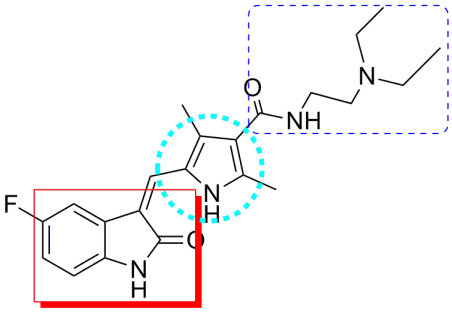

Sunitinib

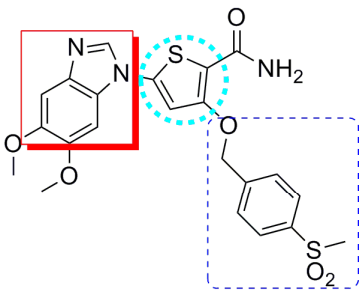

Polo-like kinase 1 (PLK1) inhibitor

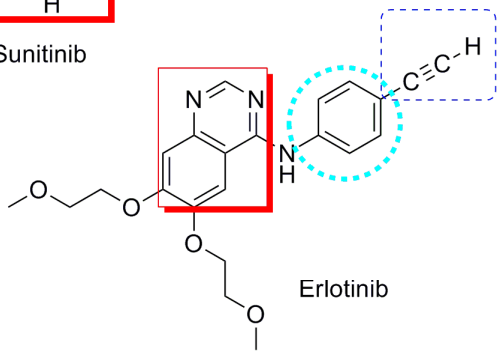

Erlotinib

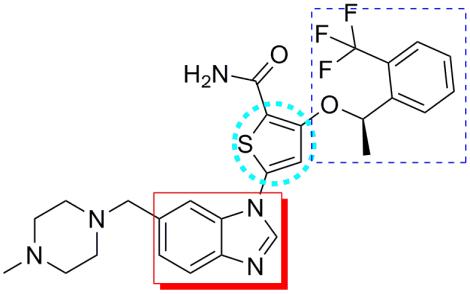

GSK461364 (PLK inhibitor)

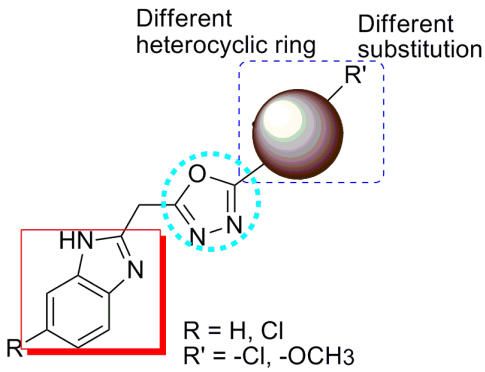

Proposed compounds (7a-x, 8a-e)

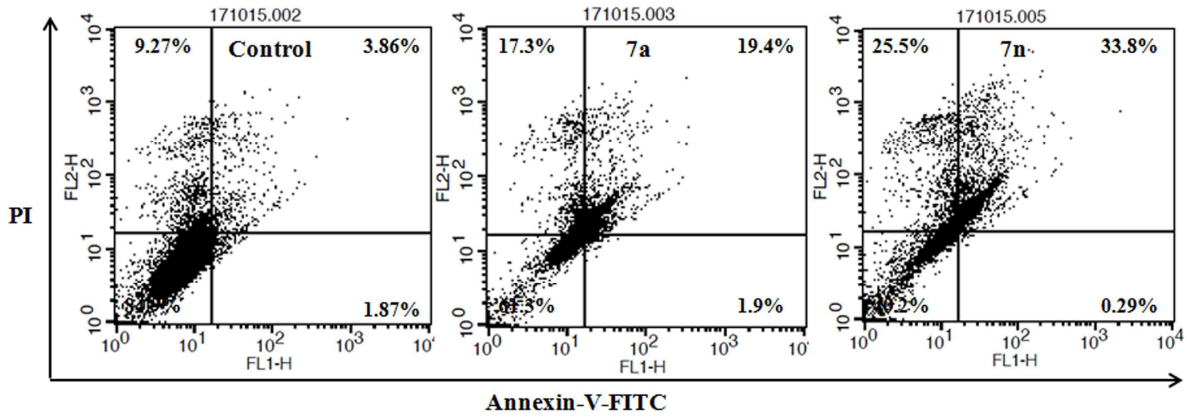

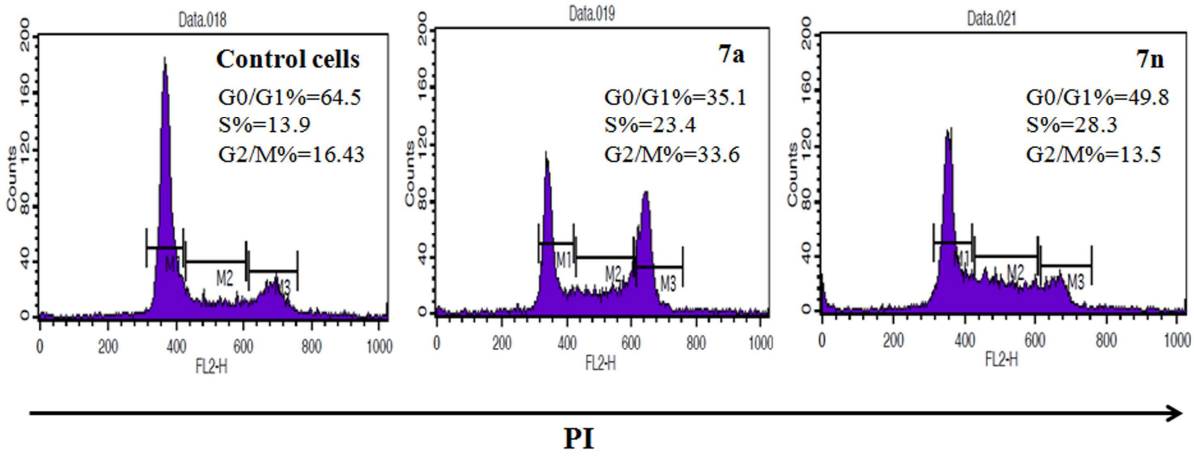

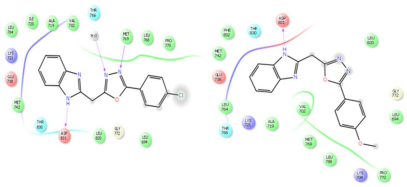

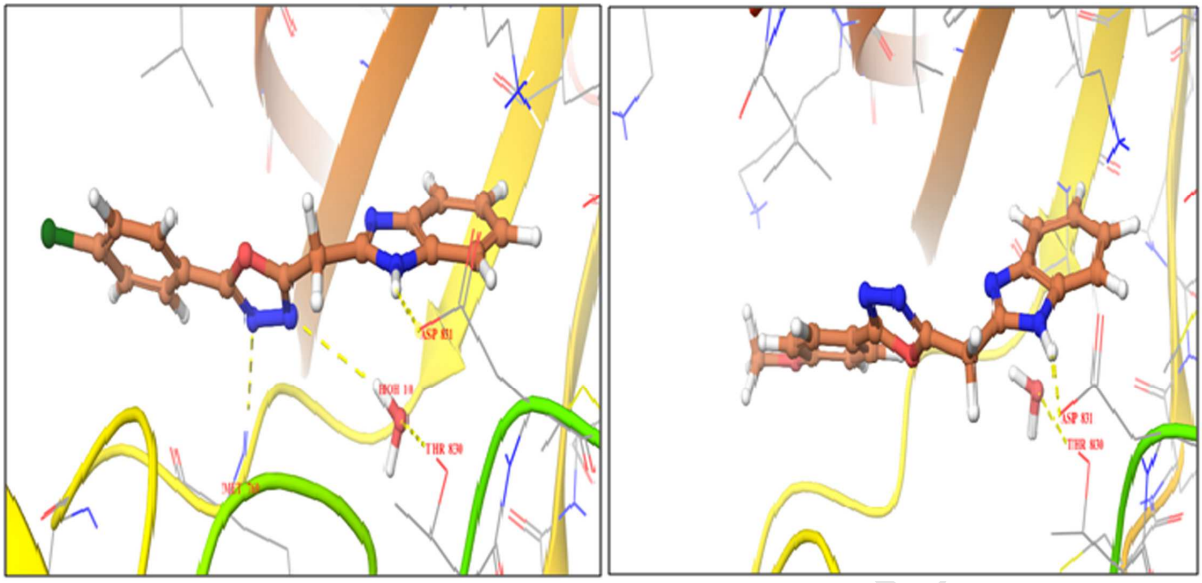

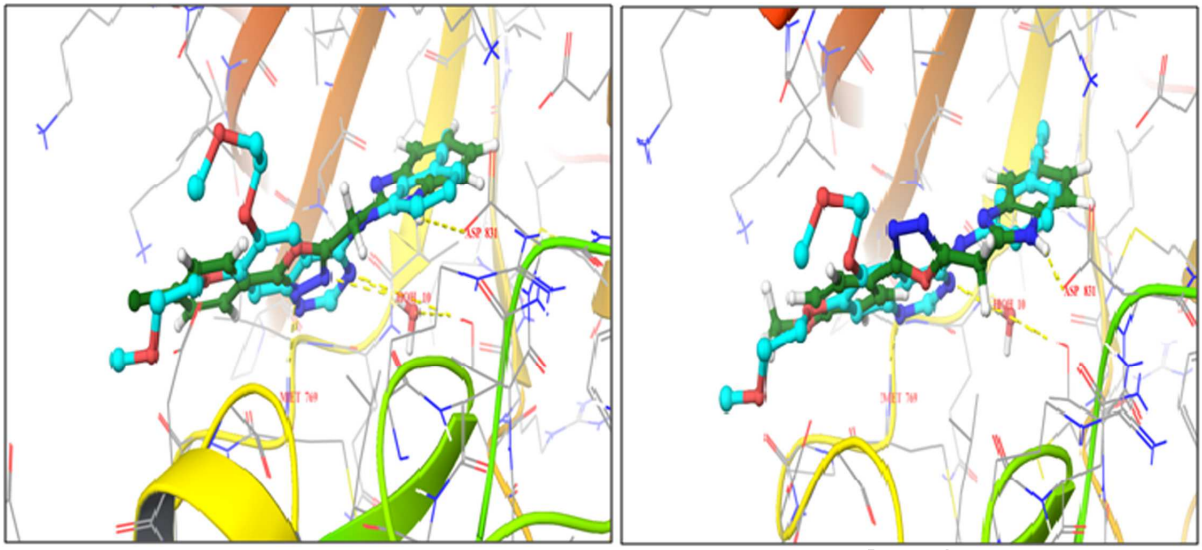

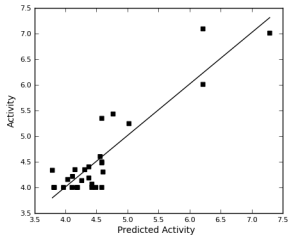

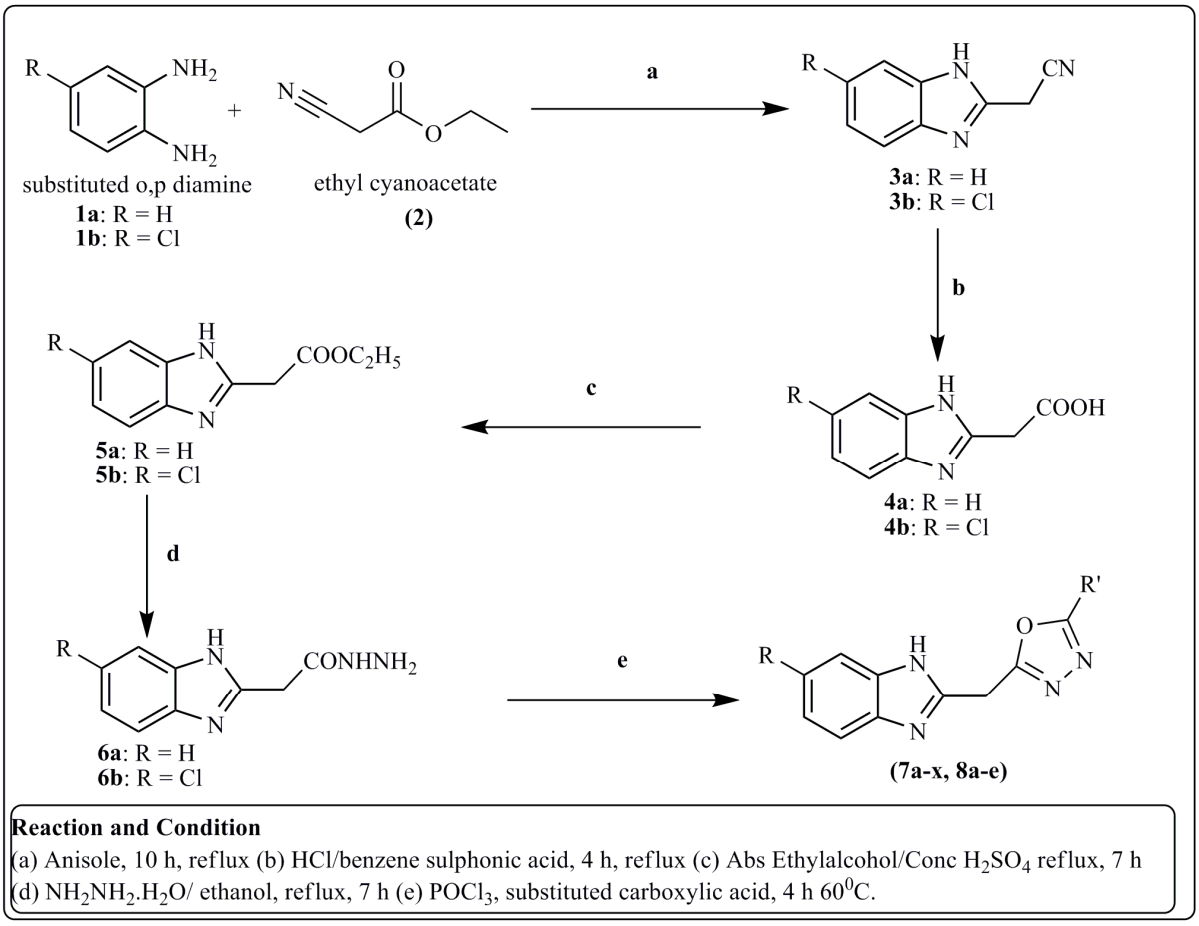

Reaction and Condition

(a) Anisole, 10 h, reflux (b) HCl/benzene sulphonic acid, 4 h, reflux (c) Abs Ethylalcohol/Conc H_2SO_4 reflux, 7 h (d) $NH_2NH_2.H_2O$/ ethanol, reflux, 7 h (e) $POCl_3$, substituted carboxylic acid, 4 h 60^0C.

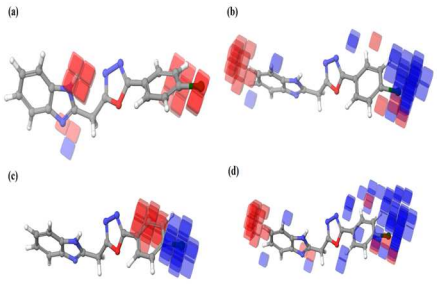

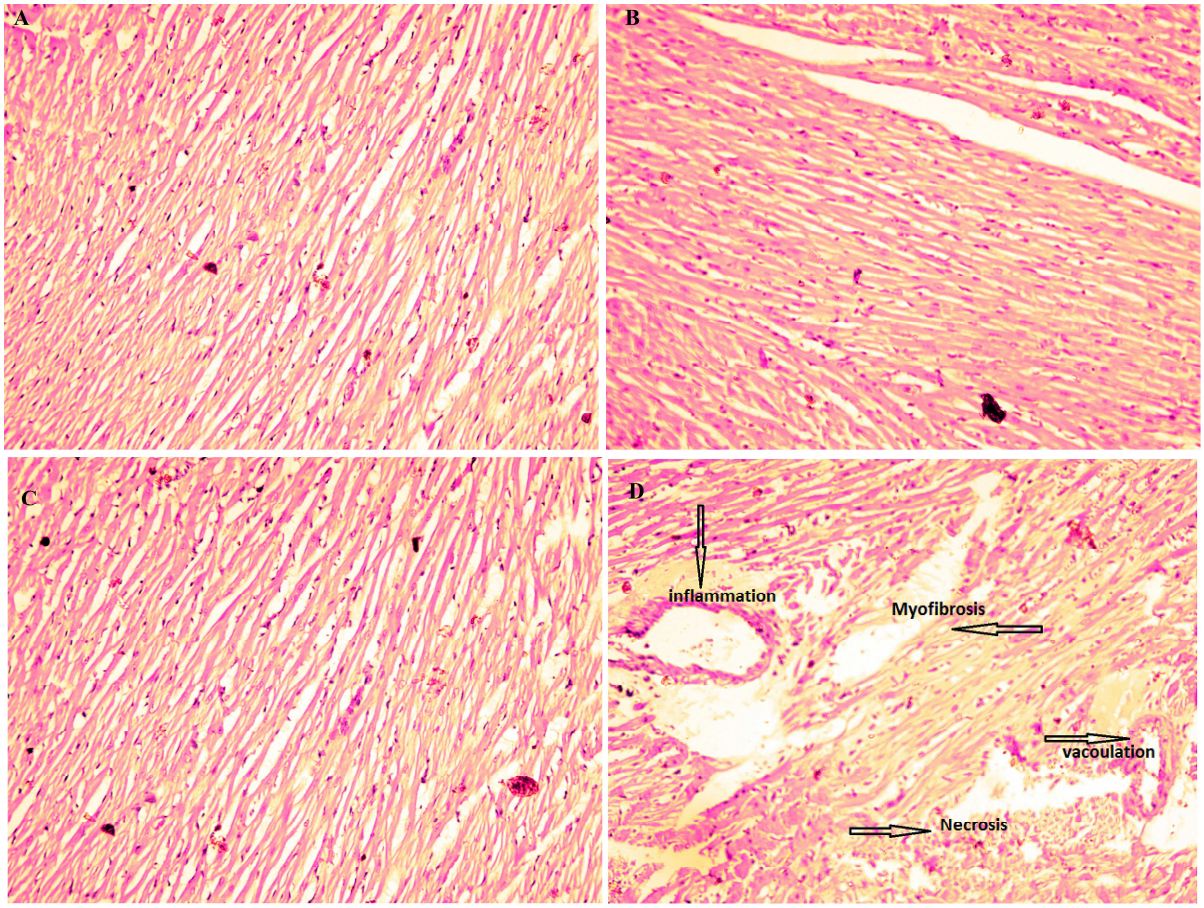

A series of twenty nine benzimidazole linked oxadizole were synthesized.

All the compounds were screened for their anticancer and *in vitro* EGFR and erbB2 receptor inhibition assay.

Two of the compounds **7a** and **7n** displayed promising activity.

The compounds **7a** showed EGFR inhibition; induce apoptosis; G2/M cell cycle arrest.

Docking and QSAR studies of the compound **7a** and **7n** are reported.